Using stability analysis of discrete elastic systems to study the buckling of nanostructures

S. N. KOROBEYNIKOV[1], V. V. ALYOKHIN[1],
B. D. ANNIN[1], A. V. BABICHEV[2]

[1] *Lavrentyev Institute of Hydrodynamics*
Lavrentyev av., 15
and
Novosibirsk State University
Pirogova str., 2, Novosibirsk, 630090, Russia
e-mail: s.n.korobeynikov@mail.ru

[2] *Sobolev Institute of Geology and Mineralogy*
Koptyug av., 3, Novosibirsk, 630090, Russia

STUBILITY/INSTABILITY CRITERIA of discrete elastic systems are used to study the buckling of nanostructures. The deformation of nanostructures is simulated by solving the nonlinear equations of molecular mechanics. The external forces applied to the nanostructure are assumed to be dead (that is the directions of their action remain constant throughout nanostructure deformation). We note that the positive-definiteness property of the tangential stiffness matrix of a nanostructure is a universal sufficient stability criterion for both equilibrium states and quasi-static/dynamic motions of the nanostructure. The equilibrium configurations are stable in Lyapunov's sense, and quasi-static/dynamic motions are stable in a finite time interval $t \in (0, T_{\mathrm{cr}})$ in which the positive-definiteness property of this matrix is preserved. For dynamic motions of nanostructures, the stability property in this time interval follows from Lee's criterion of quasi-bifurcation of solutions of second order ODEs. The non-positive definiteness of the tangential stiffness matrix of nanostructures at a time $t > T_{\mathrm{cr}}$ corresponds to both unstable equilibrium configurations and unstable dynamic motions. Computer procedures for determining the critical time and buckling mode(s) are developed using this criterion and are implemented in the PIONER FE code. This code is used to obtain new solutions for the deformation and buckling of twisted $(10, 10)$ armchair and $(10, 0)$ zigzag single-walled carbon nanotubes.

Key words: nanostructure, single-walled carbon nanotube, buckling criteria, van der Waals forces.

1. Introduction

STABILITY STUDIES OF NANOSTRUCTURE DEFORMATION are of great significance for estimating the performance of these structures. Instability of equilibrium configurations or quasi-static/dynamic motions leads to buckling of nanos-

tructures, which, as a rule, is accompanied by a sudden change in their configurations. It is therefore useful to determine the critical loads and/or times of instability of nanostructures to estimate the degree of their operational reliability. Wang *et al.* [48] analyzed existing approaches to formulating buckling problems for nanostructures and made an overview of research in this area performed up to 2010. From their analysis and review, it follows that methods of molecular dynamics (MD) (see, e.g., [31]) and molecular mechanics (MM) (see, e.g., [47]) have been extensively used to solve problems of deformation and buckling of nanostructures. The main advantage of these methods is accounting for the discrete nature of nanostructures with relative simplicity (compared to the equations of quantum mechanics and continuum mechanics) of the Newton equations of motion for material points in force fields. Among recent studies of nanostructure buckling performed using MD/MM methods, we note Ansari and Rouhi [3]; Goldstein *et al.* [17]; Huang *et al.* [20]; Kang *et al.* [21]; Khoei *et al.* [22]; Parvaneh *et al.* [39]; Sakhaee-Pour [41]; Setoodeh *et al.* [42]; Shahabi *et al.* [43]; Song and Zha [46]; Wackerfuss [47]; Wang *et al.* [49].

The MD method is simpler than the MM method, but buckling criteria for nanostructure can only be used to solve the equations of molecular mechanics. Therefore, in the present paper, we use MM equations to develop and apply buckling criteria for nanostructures. The MM equations are derived by constructing discretized equations of continuum mechanics (CM) using the finite element method (FEM). The element matrix and vector assembly routines developed for the FEM discretization of the CM equations can be used to obtain the matrices and vectors of the tangential equations of motion for nanostructures by interpreting the bonds of atoms of these nanostructures as dummy finite elements [27]. Using this analogy, Korobeynikov [25, 26]; Korobeynikov and Babichev [28]; Annin *et al.* [1, 2]; Odegard *et al.* [38]; Dluzewski and Traczykowski [12]; Li and Chou [35]; Liu *et al.* [36, 37]; Leung *et al.* [34]; Goldstein and Chentsov [16]; Goldstein *et al.* [17]; Hu *et al.* [19]; Batra and Gupta [8]; Gupta and Batra [18], Wackerfuss [47] and others applied FE codes to the solution of nonlinear deformation problems for nanostructures. In particular, Korobeynikov [25, 26]; Korobeynikov and Babichev [28]; Annin *et al.* [1] employed the PIONER FE code [24] to solve nonlinear problems of quasi-static/dynamic deformation and buckling for atomic chains, cells, and nanotubes. The present study is a further extension of the PIONER code to problems of nonlinear dynamic deformation and buckling of nanostructures, in particular, buckling and post-buckling deformation of twisted single-walled carbon nanotubes (SWCNTs).

We consider a wide class of deformation problems for nanostructures subjected to external forces whose directions remain unchanged throughout the motion (dead loads). We note that the positive-definiteness property of the tangen-

tial stiffness matrix of a nanostructure is a universal sufficient stability criterion for both equilibrium states and quasi-static/dynamic motions of the nanostructure. According to Lyapunov, stability criterion of equilibrium states with respect to dynamic perturbation introduced into a nanostructure is obtained. To determine the critical time T_{cr} such that in a time interval $t \in (0, T_{cr})$, the solution of a dynamic deformation problem of a nanostructure is stable and at a time $t > T_{cr}$ the solution is unstable, we use the stability criterion developed by Lee [33] for solutions of nonlinear second order ordinary differential equations (ODEs). According to this criterion, a solution of a system of equations is stable in a time interval in which quasi-bifurcation of this solution is absent. In the case of quasi-bifurcation, the fundamental (analyzed for stability) solution becomes unstable. At $t \approx T_{cr}$, the perturbed solution deviates sharply from the fundamental solution and then, follows a lateral quasi-branch on which the deformation mode of the nanostructure is correlated with the buckling mode obtained for the fundamental solution. Kleiber et al. [23] and Krätzig et al. [29, 30] showed that, for a system of nonlinear ODEs obtained by a finite element (FE) discretization of partial differential equations of CM, quasi-bifurcation of the solution corresponds to the time at which the tangential stiffness matrix degenerates, i.e., a dynamic instability criterion for the solution of the equations of motion of a FE ensemble is the loss of the positive definiteness property of the matrix, and the buckling mode(s) of the nanostructure are determined by zero frequency mode(s). The present paper appears to be the first in which the stability criterion developed by Lee [33], Kleiber et al. [23], and Krätzig et al. [29, 30] for solutions of the equations of dynamic motion of discrete systems is applied to buckling problems of nanostructures in a dynamic formulation.

The main objective of this study is to use the well-known instability criteria of discrete elastic systems to study the buckling of nanostructures. Although the MM equations allow the use of the above-mentioned buckling criteria of nanostructures based on the detection of singular points of integral curves of quasi-static/dynamic motions, most researchers, with rare exceptions (see, e.g., [19, 34, 36, 37, 47]), determine the critical states of nanostructures from visual observations of a sudden change in the deformation mode of nanostructures or from a decrease in the stored potential energy. However, in very accurate calculations in some cases, one may simply not notice singular points of integral curves and overestimate the performance of nanostructures. The present paper adds to and develops existing formulations of problems of nanostructure buckling, with emphasis on the determination of the critical parameters and modes of buckling immediately for unperturbed motions of nanostructures. Wang et al. [48] note "More studies are needed to fully understand the torsional buckling behavior of CNTs...". In our study, we use instability criteria of discrete elastic systems to obtain critical values for the external forces, times, and modes of

buckling of two ((10, 10) armchair and (10, 0) zigzag) SWCNTs during twisting of their ends. We found new solutions of these problems. In particular, we show how the buckling modes obtained by solving the unperturbed problem can be used to obtain their corresponding modes of initial post-critical deformation of SWCNTs.

2. Motion/equilibrium equations for nanostructures

The vector equation of motion for a nanostructure with specified initial conditions is written as follows [27]:

$$(2.1) \qquad \mathbf{M}\ddot{\mathbf{U}} + \mathbf{F}(\mathbf{U}) = \mathbf{R}, \quad \mathbf{U}(0) = \mathbf{U}_0, \quad \dot{\mathbf{U}}(0) = \mathbf{V}_0$$
$$(\mathbf{F}, \mathbf{U}, \mathbf{R}, \mathbf{U}_0, \mathbf{V}_0 \in \mathbb{R}^{\mathrm{NEQ}}, \ \mathbf{M} \in \mathbb{R}^{\mathrm{NEQ}} \times \mathbb{R}^{\mathrm{NEQ}}).$$

Here, $\mathbf{U}$, $\mathbf{F}$, and $\mathbf{R}$ are the displacement and internal and external force vectors of the nanostructure, respectively; $\mathbf{U}_0$ and $\mathbf{V}_0$ are the specified initial displacement and velocity vectors, respectively; $\mathbf{M} \succ 0$ is the diagonal mass matrix with the masses of the nanostructure atoms/molecules on the diagonal; the dot above a quantity denotes the partial derivative of this quantity with respect to time; NEQ is the total number of independent degrees of freedom of the nanostructure, i.e., the number of the scalar equations of motion in system (2.1).

If inertial forces may be neglected, Eq. (2.1) reduces to the nonlinear vector algebraic equilibrium equation (the system of NEQ scalar algebraic equations) for the nanostructure

$$(2.2) \qquad \mathbf{F}(\mathbf{U}) = \mathbf{R}.$$

Since solutions of the equilibrium equations are generally not unique, it is reasonable to reformulate the problem of definition of equilibrium of a nanostructure as the problem of quasi-static deformation by defining the sequence of all equilibrium configurations in the range from the initial to final ones. We introduce a monotonically increasing parameter τ which describes the quasi-static deformation of a nanostructure (e.g., the prescribed displacement, the arc-length of integral curve, etc.). Differentiating the left- and right-hand sides of Eq. (2.2) with respect to τ and adding initial conditions, we obtain:

$$(2.3) \qquad \mathbf{K}(\mathbf{U})\mathbf{U}' = \mathbf{R}, \qquad \mathbf{U}(0) = \mathbf{U}_0,$$

where the prime denotes differentiation with respect to the parameter τ. Here, $\mathbf{K}(\mathbf{U})$ is the tangential stiffness matrix of the nanostructure:

$$\mathbf{K} = \frac{\partial \mathbf{F}}{\partial \mathbf{U}} \ \Leftrightarrow \ K_{ij} = \frac{\partial F_i}{\partial U_j} \qquad (i, j = 1 \text{ to NEQ}).$$

We assume that all interatomic forces of the nanostructure have potential laws of interaction. Denoting the potential energy of the nanostructure by $V(\mathbf{U})$, we have:

$$\mathbf{F} = \frac{\partial V}{\partial \mathbf{U}}, \qquad \mathbf{K} = \frac{\partial^2 V}{\partial \mathbf{U} \partial \mathbf{U}},$$

i.e., the matrix $\mathbf{K}$ is a symmetric Hessian one.

Using the FEM technique, the internal force vector $\mathbf{F}$ and the tangential stiffness matrix $\mathbf{K}$ are determined by summation of the internal force vectors $\mathbf{F}^e$ and the tangential stiffness matrices $\mathbf{K}^e$ ($1 \leq e \leq M$) of all elements constituting the nanostructure

$$\mathbf{F}(\mathbf{U}) = \mathop{\mathrm{A}}_{m=1}^{M} \mathbf{F}^m(\mathbf{U}^m), \qquad \mathbf{K}(\mathbf{U}) = \mathop{\mathrm{A}}_{m=1}^{M} \mathbf{K}^m(\mathbf{U}^m).$$

Here, $\mathbf{U}^m$ is the displacement vector of the m-th element, M is the total number of nanostructure elements, and the symbol 'A' is used to denote the assembly operation [11].

In the present paper, we consider three types of nanostructure elements [1, 2, 28]: N atomic bond elements, L truss elements, and J vdW interaction elements, i.e., $M = N + L + J$. The atomic bond elements take into account the potential energy of covalent bond stretching of the atoms of the nanostructure, the truss elements take into account the potential energy of bond-angle variation, and the vdW interaction elements are due to the potential energy of noncovalent van der Waals (vdW) forces between the nanostructure(s) atoms. The potential energy of the internal forces of the nanostructure is equal to the sum of the potential energies of all its elements, i.e.,

$$V = \sum_{n=1}^{N} V_b(r_n) + \sum_{l=1}^{L} V_t(\epsilon_l) + \sum_{j=1}^{J} V_{\mathrm{vdW}}(r_j),$$

where $V_b(r_n)$ ($1 \leq n \leq N$) is the potential energy of the n-th atomic bond element, $V_t(\epsilon_l)$ ($0 \leq l \leq L$) is the potential energy of the l-th truss element, and $V_{\mathrm{vdW}}(r_j)$ ($0 \leq j \leq J$) is the potential energy of the j-th vdW interaction element; r_n and r_j are the interatomic distances between pairs of atoms, and $\epsilon_l \equiv (r_l - r_l^0)/r_l^0$ is the strain of the truss element (r_l^0 and r_l are the initial and current lengths of the l-th truss element). We denote by $V_b(r)$ the potential energy of bond stretching between the atoms in some atomic pair, by $V_t(\epsilon)$ the potential strain energy of some truss element, which approximates the potential energy of bond-angle bending, and by $V_{\mathrm{vdW}}(r)$ the potential energy of the vdW force in some atomic pair.

For the potential energy of an atomic bond element, we use the Morse potential function [9]:

$$(2.4) \qquad V_b(r) \equiv D[e^{-2\alpha(r-r_e)} - 2e^{-\alpha(r-r_e)}],$$

where D is the depth of the potential hole, r_e is the interatomic distance that corresponds to the minimum potential energy of bond stretching, and α is a specified parameter that determines the form of the potential.

For the truss elements, we use the potential strain energy function of a linear elastic material, i.e.,

$$(2.5) \qquad V_t(r) \equiv \frac{1}{2} r_0 k \epsilon^2(r), \qquad \epsilon \equiv \frac{r - r_0}{r_0}.$$

Here, k is the rigidity modulus of a truss element ($k \equiv EA$, where E is Young's modulus of the material of the truss element, and A is the cross-sectional area of this element). The role of a truss element is to simulate the contribution of the bond-angle bending energy

$$(2.6) \qquad V_\theta \equiv \frac{1}{2} k_\theta (\theta - \theta_0)^2$$

to the energy of the internal forces of the nanostructure. Here, $\theta_0 = \theta(0)$ is the initial value of the angle θ (for $t = 0$). It can be shown [16, 17, 38] that, for a small change in the angle θ ($\theta - \theta_0 \ll 1$ rad), the bond-angle bending energy (2.6) of the nanostructure is approximated by the strain energy of the truss element (2.5) with the rigidity modulus

$$k = \frac{12 k_\theta}{r_0}.$$

For the potential energy of the vdW force, we use the Lennard–Jones potential function [15]:

$$(2.7) \qquad V_{\text{vdW}}(r) = \begin{cases} 4\varepsilon \left[\left(\dfrac{\sigma}{r} \right)^{12} - \left(\dfrac{\sigma}{r} \right)^6 \right] & \text{for } 0 < r \leq r_{\text{cof}}, \\ 0 & \text{for } r > r_{\text{cof}}, \end{cases}$$

where σ and ε are prescribed constant quantities and r_{cof} is the cut-off radius.

3. Stability/instability criteria of discrete elastic system

We consider the equations of motion (2.1) for a conservative system of material particles. Let the external force be *dead* (i.e., this vector does not change its direction during deformation) such as:

$$(3.1) \qquad \mathbf{R}(t) = \lambda(t) \mathbf{R}_0,$$

where $\mathbf{R}_0$ is a constant vector that characterizes the distribution of external forces in the system and λ is a parameter that describes the intensity of the applied force.

We consider the three possible types of stability loss of solutions of the equations of system deformation:

- stability of equilibrium states of discrete elastic system with respect to dynamic perturbations,
- stability of quasi-static motions of system,
- stability of dynamic motions of system.

Below, each of these three types of instability is considered in details.

3.1. Stability of equilibrium states

Let a system be in an equilibrium state and let the equilibrium configuration with a displacement vector $\mathbf{U}$ be considered as one of the points (2.2) of the integral curve of equation (2.3). The vector equilibrium equation (2.2) taking into account Eq. (3.1) has the following form for a fixed value of the parameter τ:

$$(3.2) \qquad \mathbf{F}(\mathbf{U}) = \lambda(\tau)\mathbf{R}_0 \qquad (\tau = \text{const}).$$

Let the equilibrium state of this system be disturbed by a small perturbation, e.g., by a prescribed initial velocity $\mathbf{V}_0$. Consider the perturbed motion of the system in the vicinity of this equilibrium state. Let $\bar{\mathbf{U}}$ denote the displacement vector of the perturbed motion, so that the equation of motion (2.1) holds, i.e.,

$$(3.3) \quad \mathbf{M}\ddot{\bar{\mathbf{U}}} + \mathbf{F}(\bar{\mathbf{U}}) = \lambda\mathbf{R}_0, \quad (\lambda(\tau) = \text{const}), \quad \bar{\mathbf{U}}(0) = \mathbf{U}(\tau), \quad \dot{\bar{\mathbf{U}}}(0) = \mathbf{V}_0.$$

The motion described by equation (3.3) is assumed to develop in a natural time t. Here, the deformation parameter τ is fixed.

We introduce the notation of the deviated motion displacement vector

$$(3.4) \qquad \mathbf{q} \equiv \bar{\mathbf{U}} - \mathbf{U}.$$

Then, from Eqs. (3.2) and (3.3), we obtain the following equation with respect to the vector $\mathbf{q}$

$$(3.5) \qquad \mathbf{M}\ddot{\mathbf{q}} + \mathbf{F}(\bar{\mathbf{U}}) - \mathbf{F}(\mathbf{U}) = \mathbf{0}, \qquad \mathbf{q}(0) = \mathbf{0}, \qquad \dot{\mathbf{q}}(0) = \mathbf{V}_0.$$

Define the total energy of the system by

$$E \equiv T + e,$$

where T is the kinetic energy of the system

$$T(\dot{\mathbf{U}}) \equiv \frac{1}{2}\dot{\mathbf{U}}^{\mathrm{T}}\mathbf{M}\dot{\mathbf{U}}$$

and e is the total potential energy of the system

$$e(\mathbf{U}) \equiv V(\mathbf{U}) - \lambda \mathbf{U}^{\mathrm{T}} \mathbf{R}_0.$$

For the equilibrium configuration, we obtain

$$E(\mathbf{U}, \dot{\mathbf{U}}) = e(\mathbf{U}) = V(\mathbf{U}) - \lambda \mathbf{U}^{\mathrm{T}} \mathbf{R}_0 = \text{const},$$

and for perturbed motion we get

$$E(\bar{\mathbf{U}}, \dot{\bar{\mathbf{U}}}) = T(\dot{\bar{\mathbf{U}}}) + e(\bar{\mathbf{U}}) = T(\dot{\bar{\mathbf{U}}}) + V(\bar{\mathbf{U}}) - \lambda \bar{\mathbf{U}}^{\mathrm{T}} \mathbf{R}_0.$$

Define

(3.6) $$\Delta E \equiv E(\bar{\mathbf{U}}, \dot{\bar{\mathbf{U}}}) - E(\mathbf{U}, \dot{\mathbf{U}}) = \frac{1}{2}\dot{\mathbf{q}}^{\mathrm{T}} \mathbf{M} \dot{\mathbf{q}} + \Delta e.$$

We now find the expression for Δe:

(3.7) $$\Delta e \equiv e(\bar{\mathbf{U}}) - e(\mathbf{U}) = \mathbf{q}^{\mathrm{T}} \left(\frac{\partial e}{\partial \mathbf{U}} \right) + \frac{1}{2}\mathbf{q}^{\mathrm{T}} \left(\frac{\partial^2 e}{\partial \mathbf{U} \partial \mathbf{U}} \right) \mathbf{q} + \dots$$
$$= \mathbf{q}^{\mathrm{T}}(\mathbf{F} - \lambda \mathbf{R}_0) + \frac{1}{2}\mathbf{q}^{\mathrm{T}} \mathbf{K} \mathbf{q} + \dots = \frac{1}{2}\mathbf{q}^{\mathrm{T}} \mathbf{K} \mathbf{q} + \dots.$$

Using the smallness of $\mathbf{q}$, from Eqs. (3.6) and (3.7) we obtain:

$$\Delta E = T(\dot{\mathbf{q}}) + J(\mathbf{q}).$$

Here, we introduce the quadratic form

$$J(\mathbf{W}) \equiv \frac{1}{2}\mathbf{W}^{\mathrm{T}} \mathbf{K}(\mathbf{U}) \mathbf{W}, \qquad \mathbf{W} \in \mathbb{R}^{\mathrm{NEQ}}.$$

Let the positive definiteness condition for the quadratic form $J(\mathbf{q})$ be satisfied for the considered equilibrium configuration, i.e.,

(3.8) $$J(\mathbf{W}) \geq 0 \quad \forall \mathbf{W} \in \mathbb{R}^{\mathrm{NEQ}} \qquad \text{and} \qquad J(\mathbf{W}) = 0 \Leftrightarrow \mathbf{W} = \mathbf{0}.$$

Then,

1. $\overline{\dot{\Delta E}} = 0$ for $0 < t < \infty$;
2. $\Delta E > 0 \quad \forall \mathbf{q}, \dot{\mathbf{q}} \in \mathbb{R}^{\mathrm{NEQ}}$ ($\mathbf{q} \neq \mathbf{0}$ or $\dot{\mathbf{q}} \neq \mathbf{0}$);
3. $\Delta E = 0$ for $\mathbf{q} = \dot{\mathbf{q}} = \mathbf{0}$.

This implies that ΔE can be identified with Lyapunov's function [13]. From this it follows that Lagrange–Dirichlet Theorem can be proved using Lyapunov's second (direct) method.

Lagrange–Dirichlet Theorem (Sufficient stability conditions for the equilibrium state of a discrete elastic systems). *If the quadratic form $J(\mathbf{W})$ is positive definite, i.e., Eq. (3.8) is valid, then, the solution of Eq. (3.2) is stable according to Lyapunov.*

Remark. Proof of the Lagrange–Dirichlet Theorem using Lyapunov's direct method can be found elsewhere (see, e.g., [13, 32, 50]). Nevertheless, we believe that it is useful to give a proof of this theorem in the context of the study of the stability of solutions of the static equations of discrete elastic systems (3.2) with respect to dynamic perturbations; in this case, Eq. (3.3) is the equation of motion for the perturbed system.

Suppose that Lyapunov's stability of solution of Eq. (3.2) can be analyzed in a first approximation [14]. The stability analysis in a first approximation reduces to defining the stability of the trivial solution

$$(3.9) \qquad\qquad \mathbf{q} = \mathbf{0}$$

employing the equation

$$(3.10) \qquad \mathbf{M}\ddot{\mathbf{q}} + \mathbf{K}(\mathbf{U})\mathbf{q} = \mathbf{0}, \qquad \mathbf{q}(0) = \mathbf{0}, \qquad \dot{\mathbf{q}}(0) = \mathbf{V}_0,$$

obtained by linearization of Eq. (3.5).

The first-approximation analysis of the Lyapunov's stability of the solution of Eq. (3.10) gives no information on the stability of the reference nonlinear system if the quadratic form J is positive definite or semi-definite. If the quadratic form J is not definite (there is at least one vector $\mathbf{W} \in \mathbb{R}^{\mathrm{NEQ}}$ such that $J(\mathbf{W}) < 0$), then, solution (3.2) is unstable according to Lyapunov.

Summing up the results of the stability analysis for the solution $\mathbf{U}$ of nonlinear Eq. (3.2) by using the second Lyapunov's method and under the first approximation, we obtain the following stability criterion for this solution:

$$J(\mathbf{W}) \text{ is } \begin{cases} \text{positive definite} & (\mathbf{K} \succ 0) \\ \text{positive semi-definite} & (\mathbf{K} \succeq 0) \\ \text{undefinite} & (\mathbf{K} \not\succeq 0) \end{cases}$$

$$\Rightarrow \text{ equilibrium state is } \begin{cases} \text{stable} \\ \text{undefined} \\ \text{unstable} \end{cases}.$$

3.2. Stability of quasi-static motions

Stability analysis for the quasi-static motion of a discrete elastic system of material points is closely related to the analysis of the uniqueness of continuations

of solutions of the quasi-static deformation problem (2.3) of this system. In view of Eq. (3.2), this problem reduces to the Cauchy problem:

$$(3.11) \qquad\qquad \mathbf{K}(\mathbf{U})\mathbf{U}' = \lambda'\mathbf{R}_0, \qquad \mathbf{U}(0) = \mathbf{U}_0.$$

In turn, the analysis of the uniqueness of solutions of the problem (3.11) for some equilibrium points of the integral curve of solutions of Eq. (3.11) reduces to the determination of singular points of this curve and the determination of the status of these singular points. Thus, we now consider the problem of determining singular points of the integral curve.

DEFINITION. The points of the integral curve at which the tangential stiffness matrix degenerates, i.e., the equality

$$(3.12) \qquad\qquad\qquad\qquad \det\mathbf{K} = 0$$

is satisfied, are referred to as *singular points* [44].

We consider the scalar form of equation (3.11) [27],

$$(3.13) \qquad\qquad \mathbf{W}^\mathrm{T}\mathbf{K}(\mathbf{U})\mathbf{U}' = \lambda'\mathbf{W}^\mathrm{T}\mathbf{R}_0 \qquad \forall\,\mathbf{W} \in \mathbb{R}^\mathrm{NEQ}.$$

Let the matrix $\mathbf{K}$ be singular and $\mathbf{W}_i$ ($i = 1$ to I, $1 \leq I \leq \mathrm{NEQ}$) be the vectors forming the basis of the null-space of the matrix $\mathbf{K}$. Identifying the vector $\mathbf{W}$ in Eq. (3.13) with the vectors $\mathbf{W}_i$ in succession, we obtain the existence conditions for solutions of Eq. (3.11) at the singular point:

$$\lambda'\mathbf{W}_i^\mathrm{T}\mathbf{R}_0 = 0 \qquad (i = 1 \text{ to } I).$$

Suppose $I = 1$, i.e., the basis for the null-space of the matrix $\mathbf{K}$ consists of the unique vector $\mathbf{W}_1$. Then, the following versions are possible [45]:

$$(1)\ \lambda' = 0, \qquad \mathbf{W}_1^\mathrm{T}\mathbf{R}_0 \neq 0; \qquad (2)\ \lambda' \neq 0, \qquad \mathbf{W}_1^\mathrm{T}\mathbf{R}_0 = 0.$$

In the first case, the singular point is a turning point, and in the second case, the singular point is a bifurcation point at which two vectors $\mathbf{U}'$ corresponding to two solution continuations can be defined for one point of the integral curve [44].

Let $I > 1$; the premise is made that the singular point may be strictly coincident with a turning point and a bifurcation point [25, 26]. Assume $I = 2$; then, in this case,

$$\lambda' = 0, \qquad \mathbf{W}_1^\mathrm{T}\mathbf{R}_0 \neq 0, \qquad \mathbf{W}_2^\mathrm{T}\mathbf{R}_0 = 0.$$

Suppose that the equilibrium state of the nanostructure satisfies Eq. (3.2). The continuation of the solution from this equilibrium state satisfies Eq. (3.11). If condition (3.12) is satisfied, such an equilibrium state is called an *eigenstate*. We formulate sufficient conditions for the absence of eigenstates.

THEOREM (Sufficient conditions for the absence of eigenstates). *If the tangential stiffness matrix* $\mathbf{K}$ *is positive definite (*$\mathbf{K} \succ 0$*), i.e., Eq. (3.8) is satisfied, then, the equilibrium state is not an eigenstate.*

Let the sufficient conditions for the absence of eigenstates be satisfied for the parameter τ varying in the interval $(0, \tau_{\mathrm{cr}})$, where the value τ_{cr} corresponds to the first singular point of the integral curve. For the continuation of the solution of equations of motion through the singular point, the stability of this solution depends on the type of singularity of this point. We specify the stability status of the solution of the equations of motion depending on the type of singularity of the equilibrium point:

- $I = 1$ and the singular point is a turning point. For the continuation of the solution of equations of motion through the singular point, the solution is stable (see Fig. 1a).
- $I = 1$ and the singular point is a bifurcation point. The solution of the equations of motion is stable in the interval $(0, \tau_{\mathrm{cr}})$, and it is unstable at $\tau > \tau_{\mathrm{cr}}$ (see Fig. 1b).
- $I = 2$ and the singular point is a turning point and a bifurcation point simultaneously. The solution of the equations of motion is stable in the interval $(0, \tau_{\mathrm{cr}})$, and it is unstable at $\tau > \tau_{\mathrm{cr}}$ (see Fig. 1c).
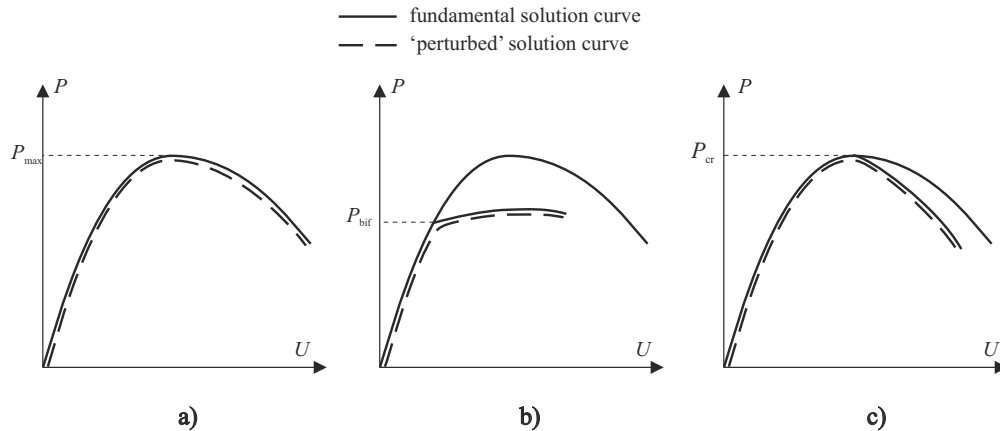

FIG. 1. Stability diagram for quasi-static motion for continuation of the solution of the equations of motion through the singular point (P is the load and U is the characteristic displacement): a) maximum load P_{max}; b) bifurcation load P_{bif}; c) maximum load with branching solution $P_{\mathrm{cr}} = P_{\mathrm{max}} = P_{\mathrm{bif}}$.

3.3. Stability of dynamic motions

To study the stability of dynamic deformation of discrete elastic system of material points, we use the definition of the stability of solutions of ODEs in the finite interval of time (see, e.g., [13]), i.e., the continuous dependence of solutions of these ODEs on the initial data (see, e.g., [14]). Let $\mathbf{U}(t)$ be a displacement vector that is the fundamental (studied for stability) solution of the equation of motion (2.1); in view of Eq. (3.1), we have:

$$(3.14) \qquad \mathbf{M}\ddot{\mathbf{U}} + \mathbf{F}(\mathbf{U}) = \lambda(t)\mathbf{R}_0, \qquad \mathbf{U}(0) = \mathbf{U}_0, \qquad \dot{\mathbf{U}}(0) = \mathbf{V}_0.$$

Let $\bar{\mathbf{U}}$ denote the displacement vector of the perturbed motion of the system that obeys the following equation of motion with perturbed initial conditions:

$$(3.15) \qquad \mathbf{M}\ddot{\bar{\mathbf{U}}} + \mathbf{F}(\bar{\mathbf{U}}) = \lambda(t)\mathbf{R}_0, \qquad \bar{\mathbf{U}}(0) = \bar{\mathbf{U}}_0, \qquad \dot{\bar{\mathbf{U}}}(0) = \bar{\mathbf{V}}_0.$$

Assuming that the vector $\mathbf{q}$ (see Eq. (3.4)) is small compared to the displacement vector $\mathbf{U}$, and using the definition of the tangential stiffness matrix, from Eqs. (3.14) and (3.15) we obtain the homogeneous equation for the vector $\mathbf{q}$:

$$(3.16) \qquad \mathbf{M}\ddot{\mathbf{q}} + \mathbf{K}(\mathbf{U})\mathbf{q} = \mathbf{0}, \qquad \mathbf{q}(0) = \mathbf{q}_0, \qquad \dot{\mathbf{q}}(0) = \mathbf{v}_0,$$

where $\mathbf{q}_0$ and $\mathbf{v}_0$ are the prescribed vectors:

$$\mathbf{q}_0 \equiv \bar{\mathbf{U}}_0 - \mathbf{U}_0, \qquad \mathbf{v}_0 \equiv \bar{\mathbf{V}}_0 - \mathbf{V}_0.$$

Using the positive-definiteness of the mass matrix $\mathbf{M}$ ($\mathbf{M} \succ 0$), from Eq. (3.16) we obtain:

$$(3.17) \qquad \mathbf{q}^{\mathrm{T}}\ddot{\mathbf{q}} = -\mathbf{q}^{\mathrm{T}}\mathbf{M}^{-1}\mathbf{K}(\mathbf{U})\mathbf{q}.$$

Lee [33] showed that the stability of dynamic motion is determined by the sign of the contraction $\mathbf{q}^{\mathrm{T}}\ddot{\mathbf{q}}$. Then, Eq. (3.17) implies that the dynamic motion is stable if the tangential stiffness matrix $\mathbf{K}$ is positive definite. Summarizing the results of investigations by Lee [33], Kleiber *et al.* [23], and Krätzig *et al.* [29, 30], we obtain the following rule for determining the interval $(0, T_{\mathrm{cr}})$ of stable dynamic motion of the system.

We assume that, at the initial time $t = 0$, the tangential stiffness matrix $\mathbf{K}$ obtained for the fundamental solution is positive definite ($\mathbf{K} \succ 0$) and remains such in a time interval $(0, T_{\mathrm{cr}})$; at the time $t = T_{\mathrm{cr}}$, the matrix $\mathbf{K}$ becomes positive semidefinite ($\mathbf{K} \succeq 0$), and at $t > T_{\mathrm{cr}}$, it is indefinite ($\mathbf{K} \not\succeq 0$). Then, the solution of Eq. (2.1) is stable in the time interval $(0, T_{\mathrm{cr}})$. At $t = T_{\mathrm{cr}}$, the stable deformation mode becomes an unstable deformation mode such that a growing nonoscillating mode in one or more perturbed motions is distinguished that

corresponds to the zero frequency eigenmode obtained by solving the generalized eigenproblem:

$$(\mathbf{K} - \mu\mathbf{M})\mathbf{\Phi} = \mathbf{0} \quad \text{at} \quad t = T_{\text{cr}}.$$

Since the matrices $\mathbf{K}$ and $\mathbf{M}$ are symmetric, the eigenvalues of the generalized eigenproblem are real. Because $\mathbf{M} \succ 0$ and $\mathbf{K} \succeq 0$, all eigenvalues are nonnegative, and we arrange them in increasing order:

$$(3.18) \qquad 0 = \mu_1 = \cdots = \mu_K < \mu_{K+1} \leq \mu_{K+2} \leq \cdots,$$

where the multiplicity K of the zero eigenvalue is equal to the deficiency of the matrix $\mathbf{K}$. Let $\mathbf{\Phi}_i$ ($i = 1$ to NEQ) be M-orthonormalized eigenvectors [7]. We arrange the eigenpairs $(\mu_i, \mathbf{\Phi}_i)$ ($i = 1$ to NEQ) according to the numbering of the eigenvalues in Eq. (3.18):

$$(\mu_1, \mathbf{\Phi}_1), \ (\mu_2, \mathbf{\Phi}_2), \ \ldots, \ (\mu_K, \mathbf{\Phi}_K), \ (\mu_{K+1}, \mathbf{\Phi}_{K+1}), \ \ldots.$$

If the solution $\bar{\mathbf{U}}$ of Eq. (3.15) is represented as the eigenmode expansion [7]:

$$(3.19) \qquad \bar{\mathbf{U}} = \sum_{i=1}^{\text{NEQ}} \alpha_i \mathbf{\Phi}_i \qquad (\alpha_i \in \mathbb{R}, \ i = 1 \text{ to NEQ}),$$

the pairs

$$(\mu_1, \mathbf{\Phi}_1), \ (\mu_2, \mathbf{\Phi}_2), \ \ldots, \ (\mu_K, \mathbf{\Phi}_K)$$

in the vicinity of the time T_{cr} determine the nonoscillating divergent [50] terms of the solution $\bar{\mathbf{U}}$ in Eq. (3.19), and the pairs

$$(\mu_{K+1}, \mathbf{\Phi}_{K+1}), \ (\mu_{K+2}, \mathbf{\Phi}_{K+2}), \ \ldots, \ (\mu_{\text{NEQ}}, \mathbf{\Phi}_{\text{NEQ}})$$

determine the contribution to this solution from the oscillating components with the frequencies

$$\omega_i = \sqrt{\mu_i} \qquad (i = K + 1 \text{ to NEQ}).$$

According to the above analysis, the zero frequency eigenmode(s) $\mathbf{\Phi}_1, \mathbf{\Phi}_2, \ldots, \mathbf{\Phi}_K$ will be called buckling mode(s), by analogy with the quasi-static analysis, and the situation in which the matrix $\mathbf{K}$ degenerates and, hence, there exists the perturbed solution (3.19) with a nonzero contribution of the zero frequency eigenmode(s) $\mathbf{\Phi}_i$ ($i = 1$ to K) to this solution will be called the quasi-bifurcation of the fundamental solution [1, 23, 29, 33].

4. Results of numerical simulation of deformation and buckling of twisted SWCNTs

The atomic bond, truss, and vdW interaction elements were implemented in the finite element library of the PIONER code [24]. In addition, the PIONER code was used to implement the algorithms for determining the quasi-static/dynamic buckling of nanostructures. Numerical solutions of the problems of deformation and buckling of SWCNTs were obtained with the help of this code. Pre- and post-processing of these solutions were performed using the MSC.Patran 2010 code [6]. The problems of quasi-static or dynamic nanotube deformations were solved by step-by-step integration of the MM equations of quasi-static or dynamic motion, in the latter case we used the Newmark method [7]. In each integration step, the solution was refined using the iterative procedure of the Newton–Raphson method [7].

The constants of the potential functions (2.4), (2.6), and (2.7) for SWCNTs have the following values [9, 15]:

$$r_e = 0.142 \text{ nm}, \qquad \alpha = 26.25 \text{ nm}^{-1}, \qquad D = 0.603105 \text{ nN} \cdot \text{nm},$$

$$k_\theta = 0.9 \text{ nN} \cdot \text{nm/rad}^2, \qquad \sigma = 0.3412 \text{ nm}, \qquad r_{\text{cof}} = 0.45 \text{ nm},$$

$$\varepsilon = 0.0003840 \text{ nN} \cdot \text{nm}, \qquad m_a = 0.019927 \text{ nN} \cdot \text{ps}^2/\text{nm},$$

where m_a is the mass of the carbon atom.

It is known that the tangential stiffness of vdW forces is negligibly small compared to the tangential stiffness of covalent bonds (less than one percent [16]). Therefore, for saving computation time, the vdW forces between any atom considered and the chemically (covalently) bonded atoms at the four nearest bond levels with this atom were neglected in this study[1]. We included vdW forces primarily to prevent intersections of the external and internal "surfaces" of nanotubes under large post-critical deformations. The value of the cut-off radius $r_{\text{cof}} = 0.45$ nm (see (2.7)) used in this study corresponds to the inclusion of attractive vdW forces of large magnitudes and repulsive vdW forces of any magnitude. In the determination of bifurcation/quasi-bifurcation points and their corresponding buckling modes of nanotubes, vdW forces are not considered to save computational resources. However, in the solution of problems of post-critical deformation of SWCNTs, the action of vdW forces is taken into account.

4.1. Deformation and buckling of a (10,10) armchair SWCNT

To demonstrate the usefulness of using the stability/instability criteria of discrete elastic systems to study nanostructure buckling, we solve the problem

---

[1]For details of the strategy of including or ignoring vdW forces in the present work, see [2].

of deformation and buckling of a $(10, 10)$ armchair SWCNT and compare the obtained solution with the solution of this problem given in [4]. In the cited paper, the problem of quasi-static deformation of the SWCNT was obtained by the MM method. In [4], the critical values of the twisting angle corresponding to the SWCNT buckling were determined from the condition that the potential energy of the internal forces on the nanotube reaches a local maximum with monotonically increasing twisting angle.
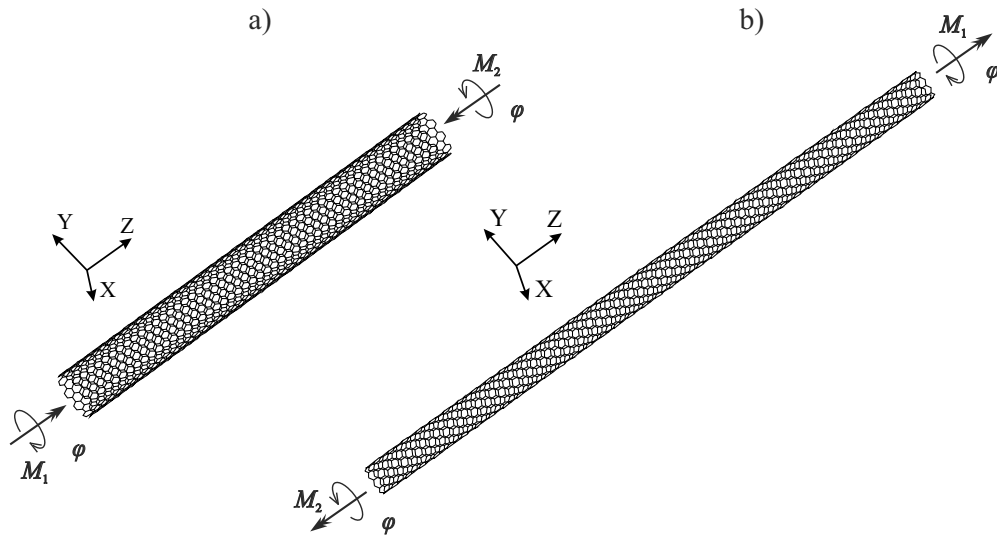

FIG. 2. Two twisted SWCNTs: a) a $(10, 10)$ armchair SWCNT; b) a $(10, 0)$ zigzag SWCNT.

Consider an armchair type SWCNT [40] with chirality indices $(10, 10)$ of radius $R = 0.6792$ nm and length $L = 12.2919$ nm (50 hexagonal cells in its length). The atoms at both edges of the SWCNT are constrained in the axial direction and move on circles of radius R with prescribed monotonically increasing twisting angle φ (Fig. 2a). The torques M_1 and M_2 at the edges are found from the values of the reaction forces for the atoms at the edges of the nanotube in solving the problem. Since, in the static analysis, there are no other external forces except for the torques M_1 and M_2, the static equilibrium conditions imply that $M = M_1 = M_2$, as was confirmed in our numerical solution of the quasi-static deformation problem. In the dynamic analysis, this equality can be violated due to the presence of inertial forces. Nevertheless, in the numerical solutions corresponding to the fundamental solution (corresponding to nanotube deformation without folding) of the dynamic problem of nanotube twisting, the equality $M = M_1 = M_2$ is also preserved. Thus, henceforth, at the bifurcation and quasi-bifurcation points, we give only one critical value $M_{cr} = M_{1,cr} = M_{2,cr}$ of the torque.

Numerical experiments in solving the unperturbed problem[2)] of quasi-static deformation of the SWCNT for various values of $\Delta\varphi$ showed that the critical angle φ_{cr} corresponding to the first bifurcation point(s) of the integral curves (see Fig. 3 a,b) is determined sufficiently accurately by integrating the equations of quasi-static deformation with a twisting angle step $\Delta\varphi = 0.05625°$. In this case, the elements of the diagonal matrix $\mathbf{D}$ in the expansion $\mathbf{K} = \mathbf{L}\mathbf{D}\mathbf{L}^T$ (the matrix $\mathbf{L}$ is the lower unit triangular matrix) [7] change sign(s) from positive to negative[3)]. We note that with the first change of the sign(s) of element(s) of the matrix $\mathbf{D}$, the matrix $\mathbf{K}$ loses positive-definiteness (in the range of the twisting angle φ from zero to the lower value φ_{cr} the matrix $\mathbf{K}$ is positive definite). According to the instability criteria of discrete elastic systems, all deformed configurations of the nanotube in the range of the twisting angle $\varphi \in (0°, \varphi_{cr,1})$ ($\varphi_{cr,1}$ is the value of the monotonically increasing angle φ at the first singular point on the integral curve) are in stable equilibrium states with respect to dynamic perturbations, and for $\varphi > \varphi_{cr,1}$ they are in unstable equilibrium states (see Sec. 3.1). Stability of quasi-static motion is provided only in this range of the angle φ (see Sec. 3.2). We obtain the first two bifurcation points on the integral curve for the dependence of the torque $M(= M_1 = M_2)$ on the twisting angle φ of the fundamental solution: ($\varphi_{cr,1} = 1.5188°$, $M_{cr,1} = 1.2825 \text{ nN} \cdot \text{nm}$) and ($\varphi_{cr,2} = 2.4750°$, $M_{cr,2} = 2.0887 \text{ nN} \cdot \text{nm}$). These points correspond to the lower values of φ and M in the intervals containing the bifurcation points. The buckling modes of the nanotube obtained at these bifurcation points on the integral curve of the fundamental solution are depicted in Fig. 3c, d.

In the present work, we were not able to obtain solutions of the problems of post-critical quasi-static deformation of SWCNTs. In order to obtain post-critical deformed configurations, we modeled quasi-static deformation by dynamic one using the twisting angle φ which is sufficiently extended in time. By the regime of nanotube twisting which is "sufficiently extended in time" we understand the regime in which, first, the first quasi-bifurcation point(s) of the fundamental solution of the dynamic nanotube deformation problem is(are) close to the first bifurcation point(s) of the fundamental solution of the quasi-static deformation of the same nanotube, second, the buckling modes coincide in both cases, and third, we can obtain converged solutions in the range of the twisting angle φ from zero to 360°. Numerical experiments established that the deformation regime which is sufficiently extended in time occurs when the nanotube is twisted at a rate $\dot{\varphi} = 1.8°/\text{ps}$; in this case, the atoms at both edges of the nanotube make a full turn (i.e., $\varphi = 360°$) in a time $T = 200$ ps. We note that attempts to use defor-

---

[2)]The term unperturbed problem is defined below in this section.

[3)]Change of signs(s) of element(s) of the matrix $\mathbf{D}$ in a certain range of the angle φ indicates that this interval of the integral curve contains singular point(s) (see Sec. 3.2) [25].
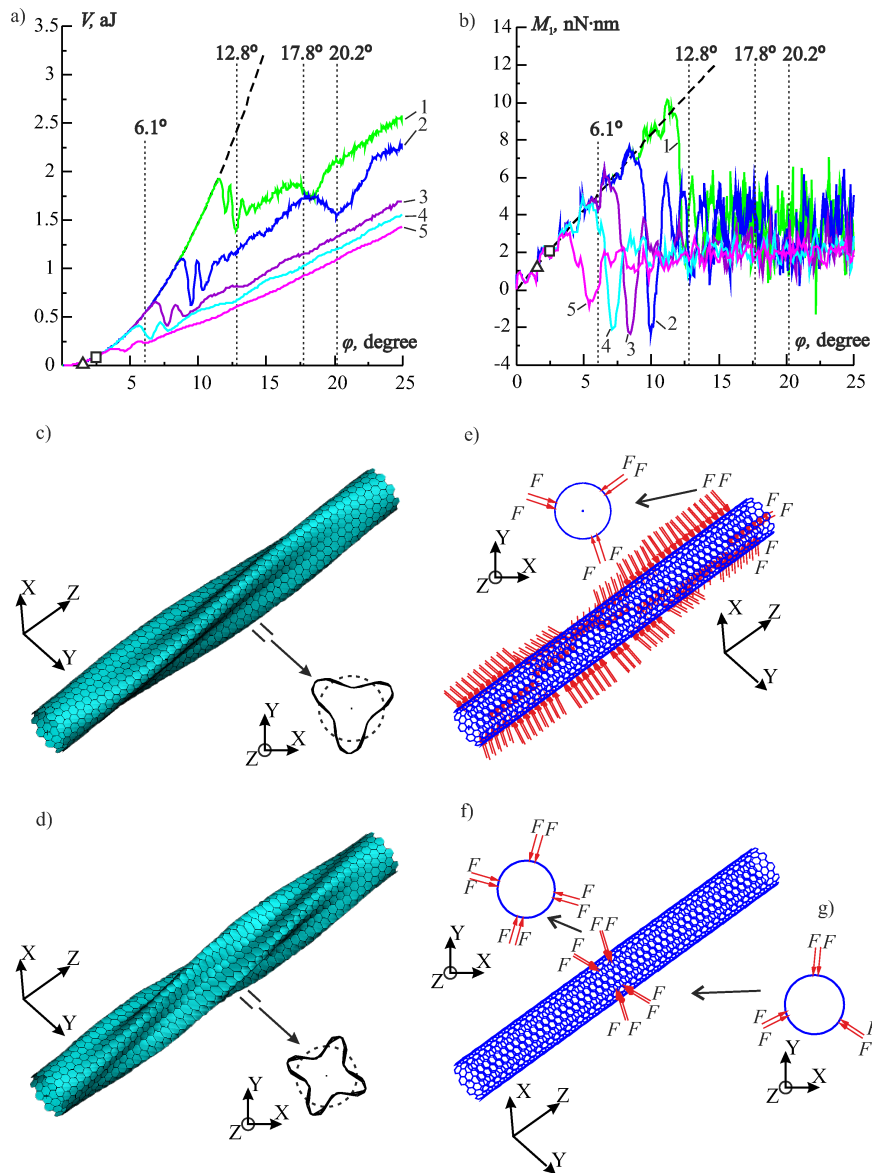
FIG. 3. Deformation and buckling of the twisted $(10, 10)$ armchair SWCNT: a), b) potential energy of internal forces V and torque M_1 versus twisting angle φ (dashed curves correspond to the solution of the quasi-static problem, and solid curves correspond to the solutions of the dynamic problems for $\dot{\varphi} = 1.8\,°/\text{ps}$); solid curves #1 correspond to the solution of the unperturbed problem, and solid curves #2, #3, #4, #5 correspond to the solutions of the problem with perturbations of types #1, #2, #3, #4; c), d) buckling modes obtained at the (quasi-)bifurcation points in the solution of the unperturbed problem, which are marked by '△' and '□', respectively, in a) and b); e) helical distribution of the perturbing compression forces acting on the atoms of the SWCNT and fitted to the buckling mode in c); f), g) circular distribution of the perturbing compression forces fitted to: f) the buckling mode in d); g) the buckling mode in c).

mation regimes that are even more extended in time have not given converged solutions over the entire range of the twisting angle φ from zero to 360°. To obtain quasi-bifurcation points and corresponding buckling modes, the solution of the dynamic unperturbed problem (ignoring vdW forces) was performed with the same step of the twisting angle ($\Delta\varphi = 0.05625°$) as the solution of the similar quasi-static problem. As a result, we obtained quasi-bifurcation points and their corresponding buckling modes which coincide with the bifurcation points and their corresponding buckling modes obtained from the solution of the problem of quasi-static deformation of the nanotube (see Fig. 3a–d).

In accordance with the approach presented in [25, 26], to find the post-critical deformed configurations, we must subject nanostructure deformation to a small perturbation, possibly agreeing with the buckling mode(s) obtained at the (quasi-)bifurcation point on the integral curve of the solution. Henceforth, by solutions of the unperturbed problem we understand solutions obtained for the initial positions of atoms in the nanostructure specified by using double precision arithmetic; furthermore, for the initial configuration of the nanotube, the interatomic distances r_e are specified with a minimum accuracy of 13 significant digits. By solutions of the problem with type #1 perturbation we understand solutions obtained for the initial positions of atoms in the nanostructure specified using up to the first five significant digits (i.e., simulating calculations using single precision arithmetic), and by solutions of problems with perturbations of types #2, #3, and #4 we understand solutions of problems obtained with specified additional compression forces applied to the atoms in a helix along the axial coordinate of the nanotube which have absolute values $F = 10^{-5}$, 10^{-4}, 10^{-3} nN, respectively (see Fig. 3 e). These additional forces are indeed perturbing because when the twisting torque reaches a value $M_{\mathrm{cr},1} = 1.2825$ nN $\cdot$ nm, the average value of the reaction forces acting on the atoms is approximately, 0.118 nN, i.e., the largest value of the perturbing forces ($F = 10^{-3}$ nN) is two orders of magnitude smaller than the average value of the reaction forces acting on the atoms located at the edges of the SWCNT. Thus, perturbations of type #1 are random in nature, and perturbations of types #2, #3, and #4 cause post-critical motions of the nanotube with deformed configurations correlated with the lower buckling mode (see Fig. 3c). Since the first lower (quasi-)bifurcation points are close to each other (see Fig. 3a, b), one can expect the development of post-critical deformation modes correlated with both the 3-half-wave buckling mode (see Fig. 3c) and the 4-half-wave one (see Fig. 3d). To purposefully cause post-critical deformation of the nanotube correlated with the 4-half-wave buckling mode, we introduce a system of perturbing forces distributed on the circle of the nanotube and fitted to the 4-half-wave buckling mode (see Fig. 3f). By solutions of the problem with perturbations of types #5, #6, and #7 we mean solutions obtained with the use of specified additional compression forces

which act on the atoms on the circle of the nanotube as shown in Fig. 3f and have absolute values $F = 10^{-5}$, 10^{-4}, 10^{-3} nN, respectively. In addition, for an additional study of the effect of the spatial distribution of the perturbing forces on the modes of deformed configurations, we introduce a system of perturbing forces distributed on the circle of the nanotube and fitted to the 3-half-wave buckling mode (see Fig. 3g). By solutions of the problem with perturbations of types #8, #9, and #10 we mean solutions obtained with the use of specified additional compression forces which act on the atoms on the circle of the tube as shown in Fig. 3g and have absolute values $F = 10^{-5}$, 10^{-4}, 10^{-3} nN, respectively.

As noted above, we obtained bifurcation/quasi-bifurcation points and their corresponding buckling modes of the SWCNT ignoring the vdW forces of interatomic interactions. The solutions given below for the problems of determining deformed configurations for dynamic motions of the nanotube, including post-critical deformation, were obtained taking into account the vdW forces. In the numerical experiments, we found a time step $\Delta t = 0.00625$ ps with $\Delta \varphi = 0.01125°$ that ensured the convergence of the solutions up to a twisting angle of $360°$. The results of simulating the dynamic deformation of a twisted nanotube for solving both the unperturbed problem and the problems with perturbations of types ##1-10 are depicted in Figs. 3–9. The graphs of the torques M_1 and M_2 versus φ differ insignificantly at scales of Figs. 3b, 4b, and 5b. Thus, we show only the dependence of the torque M_1 on φ.

We observe two qualitatively different configuration modes for initial post-critical deformation of the nanotube; that is, the configuration modes for initial post-critical deformation obtained by solving the unperturbed problem and the problems with perturbations of types #1, #5, #6, and #7 correlate with the 4-half-wave buckling mode presented in Fig. 3d (see the post-buckling configuration obtained by solving the unperturbed problem and presented in Fig. 6a for a twisting angle $\varphi = 12.8°$), and the configuration modes for initial post-critical deformation obtained by solving the problems with perturbations of types #2, #3, and #4 correlate with the 3-half-wave buckling mode presented in Fig. 3c (see the post-buckling configuration obtained by solving the problem with perturbations of type #4 and presented in Fig. 6b for a twisting angle $\varphi = 6.1°$). From the graphs depicted in Fig. 3a, b it is evident that the smaller the perturbation parameter, the farther from the first quasi-bifurcation point the curve of the post-critical deformation solution "branches" away from the curve of the fundamental solution (from $\varphi = 3.8°$ for the solution to the problem with perturbations of type #4 to $\varphi = 11.5°$ for the solution to the unperturbed problem). The points of "branching" away from the fundamental solution were determined by the internal forces energy V reaching the local maximal values. One can see that the initial segments of the curves "branching" away from the fundamen-
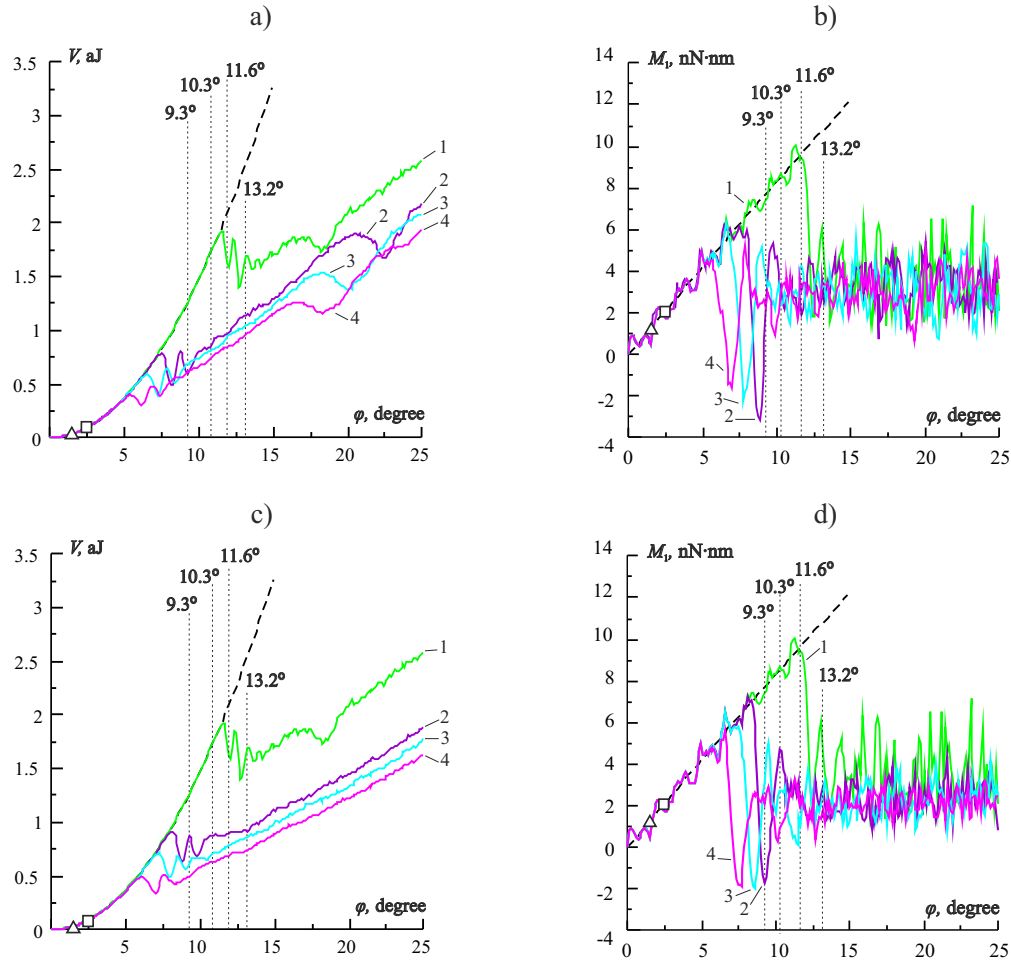
a)

b)

c)

d)

Fig. 4. Potential energy of internal forces V and torque M_1 versus twisting angle φ for the twisted $(10, 10)$ armchair SWCNT (dashed curves correspond to the solution of quasi-static problem, and solid curves correspond to the solutions of dynamic problems for $\dot{\varphi} = 1.8\,°/\text{ps}$): a), b) curves #1 correspond to the solution of the unperturbed problem, and curves #2, #3, and #4 correspond to the solutions of the problem with perturbations of types #5, #6, and #7 (circular distribution of the perturbing compression forces fitted to the 4-half-wave buckling mode, see Fig. 3d); c), d) curves #1 correspond to the solution of the unperturbed problem and curves #2, #3, and #4 correspond to the solutions of the problem with perturbations of types #8, #9, and #10 (circular distribution of the perturbing compression forces fitted to the 3-half-wave buckling mode, see Fig. 3c).

tal solution correspond to the solution of the post-critical deformation problem without oscillations (i.e., on this segment, the solution is of divergence type [50]). According to the stability criterion of dynamic motions of discrete elastic systems (see Sec. 3.3), stable dynamic motion of the nanotube occurs in the range of the twisting angle $\varphi \in (0°, \varphi_{\text{cr},1} = 1.5188°)$, and outside this range, the fundamental
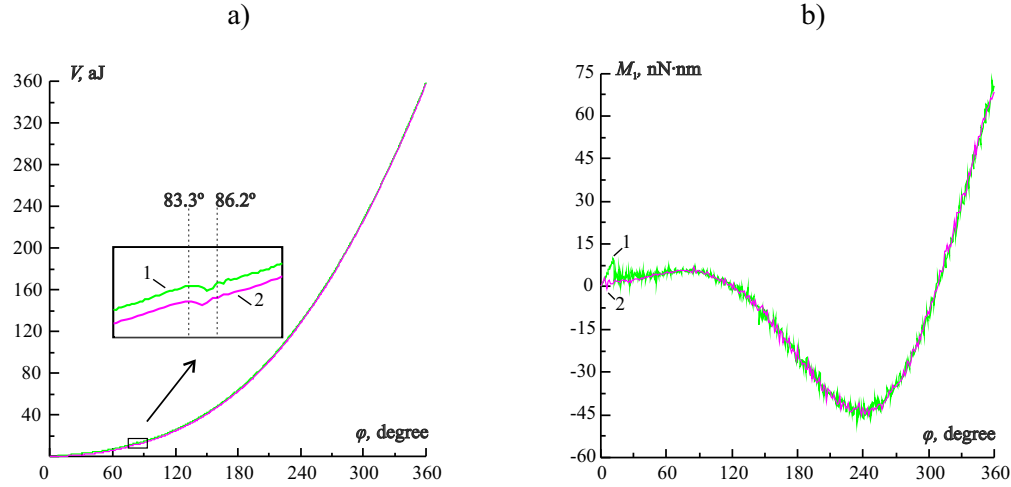
FIG. 5. Potential energy of internal forces V and torque M_1 versus twisting angle φ (curves #1 correspond to the solution of the unperturbed problem, and curves #2 correspond to the solution of the problem with perturbations of type #4) for dynamic deformation of the twisted $(10, 10)$ armchair SWCNT for $\dot{\varphi} = 1.8\,^\circ/\text{ps}$.

solution corresponding to the dynamic motion of the nanotube without folding is unstable.

We note that the curves of the potential energy of internal forces V and torque M_1 versus twisting angle φ for fairly large values of this angle ($\varphi > 15°$) are close to each other (see Fig. 5), but the changes in the modes of deformed configurations follow different patterns depending on the modes of initial post-critical deformation (correlated with the 3- or 4-half-wave buckling modes). Ultimately, for fairly large twisting angles ($\varphi \gtrsim 86.2°$), the modes of post-critical deformation correspond to fully flattened modes, but this transformation of the helical 4-half-wave post-buckling modes to fully flattened modes occurs much earlier than the similar transformation of the 3-half-wave post-buckling modes to fully flattened modes. Local maxima in the curves of the potential energy of internal forces V versus twisting angle φ in the range $15° < \varphi < 25°$ for the solutions of the unperturbed problem and problems with perturbations of type #1 (see Fig. 3a) and with perturbations of types #5, #6, and #7 (see Fig. 4a) suggest that in this range of the twisting angle, the post-critical deformation of the nanotube corresponding to the 4-half-wave post-buckling mode undergoes catastrophic transformations. Indeed, an analysis of changes in the deformed configurations obtained in the solution of, e.g., the unperturbed problem shows that in the range of the angle $17.8° < \varphi < 20.2°$ (see Fig. 3a), the helical 4-half-wave post-buckling mode is transformed into the fully flattened mode (see Fig. 6a). At the same time, curves of the potential energy of internal forces V versus twisting angle φ, obtained by solving the problem with perturbations of

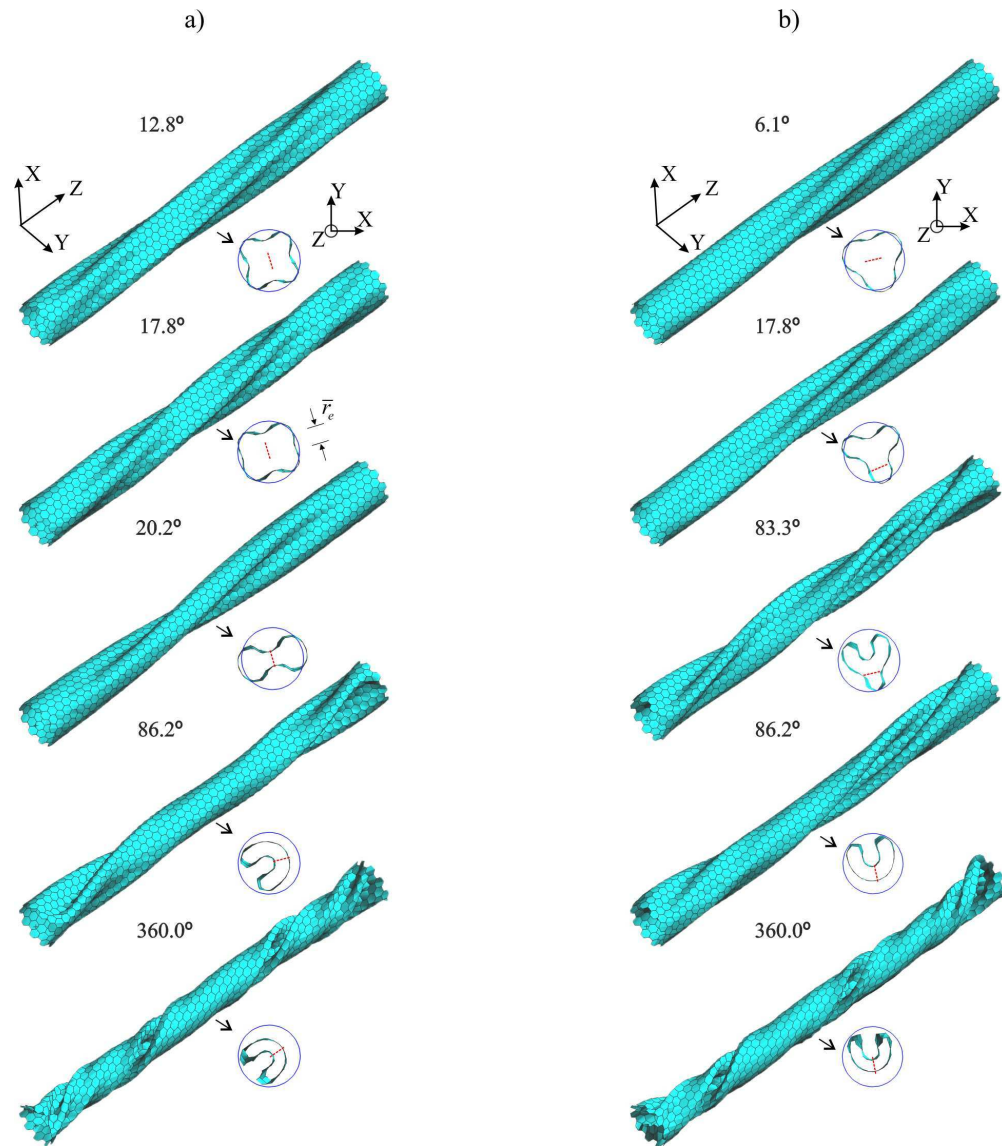a)   b)

FIG. 6. Post-buckling configurations of the twisted $(10, 10)$ armchair SWCNT under dynamic deformation for $\dot{\varphi} = 1.8\,^{\circ}$/ps (values of the twisting angle φ are given near the deformed configurations) corresponding to the solutions of: a) the unperturbed problem; b) the problem with perturbations of type #4.

types #2, #3, and #4 do not have local maxima at angles $15° < \varphi < 25°$ (see Fig. 3a). An analysis of the modes of deformed configurations obtained for these solutions shows that, in this range of the twisting angle, the nanotube continues to deform according to the helical 3-half-wave post-buckling mode (see Fig. 6b).

Transformation of these post-buckling modes into the fully flattened modes for the solutions of the problem with perturbations of types #2, #3, and #4 occurs in the range of the angle $83.3° < \varphi < 86.2°$ (an example of such transformations for the solution of the problem with perturbations of type #4 is presented in Fig. 6b). In this range, the curve of the potential energy of internal forces V versus twisting angle φ has a local maximum (an example of such a local maximum obtained by solving the problem with perturbation of type #4 is presented in Fig. 5a). Similar curves of the potential energy of internal forces V versus twisting angle φ are obtained for the solutions of the problem with perturbations of types #2 and #3. We note that the ranges of the twisting angles corresponding to the transformations of the helical 3-half-wave post-buckling modes into the fully flattened mode include the turning points of integral curves of the torque M_1 versus twisting angle φ (see Fig. 5b). We also note that in the range of the angle $83.3° < \varphi < 86.2°$, the curves of the potential energy of internal forces V versus twisting angle φ for the solutions of the unperturbed problem (see Fig. 5a) and the problem with perturbations of types #6 and #7 also reach local maxima, but in this case, the modes of post-critical deformations do not undergo qualitative changes and continue to remain fully flattened modes of the same form (see Fig. 6a). These local maxima of the potential energy might be related to the fact that the integral curves of the torque M_1 versus twisting angle φ reach turning points (see the integral curve in Fig. 5b for the solution of the unperturbed problem). However, in this range of the angle φ, the curves of the potential energy of internal forces V versus twisting angle φ for the solutions of the problem with perturbations of types #1 and #5 do not have local maxima although the integral curves of the torque M_1 versus twisting angle φ reach turning points in the same range. Thus, in the range $83.3° < \varphi < 86.2°$, the curves of the potential energy of internal forces V versus twisting angle φ for the solutions of both the unperturbed problem and the problem with perturbations of types #2, #3, #4, #6, and #7 reach local maximum; furthermore, in this range, the integral curves of the torque M_1 versus twisting angle φ reach turning points, but only the modes of deformed configurations obtained by solving the problem with perturbations of types #2, #3, and #4 undergo qualitative transformations from the helical 3-half-wave post-buckling modes into fully flattened modes. An analysis of the deformed configurations shows that in the range of the twisting angle $86.2° < \varphi < 360°$, regardless of the form of the initial helical post-buckling mode, the nanotube has the form of a "twisted ribbon" or, in other words, it is a fully collapsed (flattened) SWCNT [10]. This ribbon is hollow and the distance between its walls is about $\bar{r}_e = \sqrt[6]{2}\sigma = 0.3830$ nm, i.e., at this distance, the attractive and repulsive constituents of the vdW forces are equilibrated (see Fig. 6). However, this ribbon does not have the symmetry property about the middle of the nanotube. By rotating the deformed nanotube
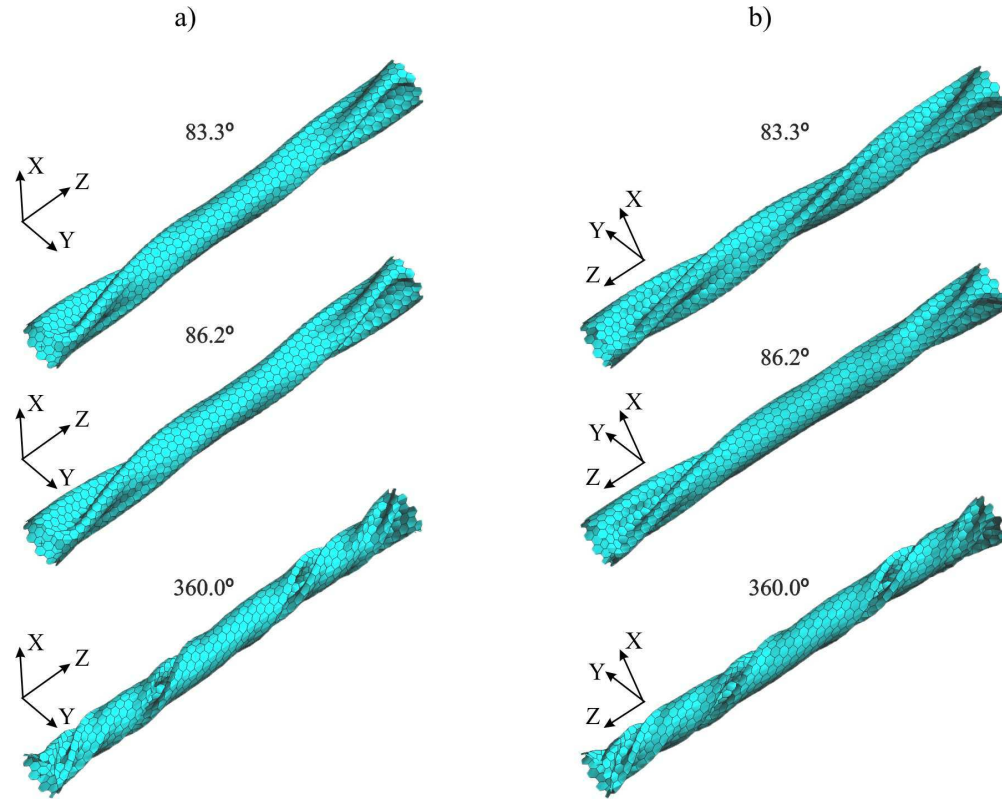
Fig. 7. Post-buckling configurations of the twisted $(10, 10)$ armchair SWCNT under dynamic deformation for $\dot{\varphi} = 1.8\,°/\text{ps}$ obtained in the range of the twisting angle $83.3° < \varphi < 360°$ (values of the twisting angle φ are given near the deformed configurations): a) solution of the unperturbed problem; b) solution of the problem with type #4 perturbations.

configurations for the problem with perturbation of type #4 so as to interchange the upper and lower edges by choosing angles of observation of the SWCNT, it can be shown that the deformed configurations of the nanotube obtained by solving the unperturbed problem and the problem with type #4 perturbations in the range of the twisting angle $86.2° < \varphi < 360°$ are identical (see Fig. 7). It is also evident (see Fig. 7) that the deformed configurations of the nanotube obtained by solving the unperturbed problem and the problem with perturbations of type #4 differ from each other for a twisting angle $\varphi = 83.3°$ (at this twisting angle, the mode of deformed configuration of the nanotube obtained by solving the unperturbed problem corresponds to the fully flattened mode and the mode of deformed configuration obtained by solving the problem with type #4 perturbations corresponds to the helical 4-half-wave post-buckling mode).

We note that perturbing forces of types #8, #9, and #10 fitted to the 3-half-wave buckling mode are weaker than perturbing forces of types #2, #3, and
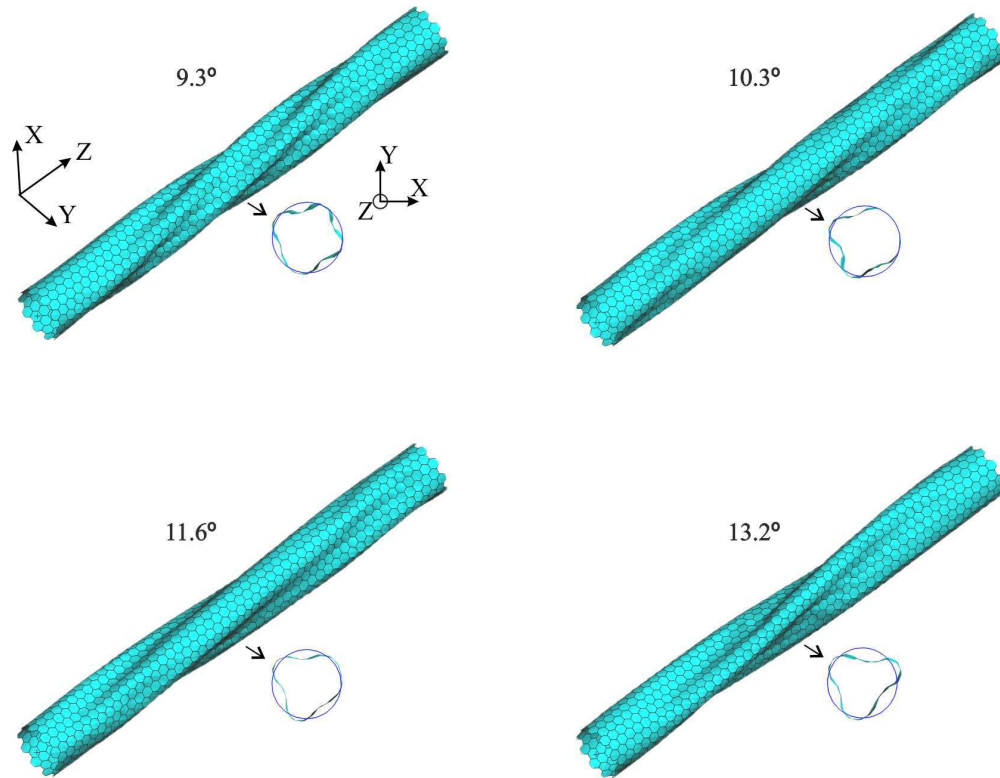
Fig. 8. Transformation of 4-half-wave post-buckling modes to 3-half-wave post-buckling modes (values of the twisting angle φ are given near the deformed configurations) obtained by solving the problem of twisting of the $(10, 10)$ armchair SWCNT under dynamic deformation for $\dot{\varphi} = 1.8\,°/\text{ps}$ with type #8 perturbations (see curves #2 in Fig. 4 c,d).

#4 fitted to the same buckling mode. This may explain the fact that the modes of initial post-critical deformed configurations obtained by solving the problem with perturbations of these types correlate with the 4-half-wave buckling mode. However, during further twisting (recall that the perturbing forces are constant in time), these modes of post-critical deformation are rapidly transformed to the 3-half-wave post-buckling modes (see Figs. 8, 9) and the further post-buckling deformation of the nanotube with perturbations of these types follow the scenario of the post-critical deformation of the nanotube with perturbations of types #2, #3, and #4.

Let us compare the obtained solutions with the solutions of the same problem presented by ARROYO and BELYTSCHKO [4]. In the paper cited, the maximum twisting angle of the nanotube was set equal to $\varphi = 25°$. The authors considered two solutions of the problem of twisting of the nanotube by the MM method. In the solution of the unperturbed problem, the critical twisting angle was found
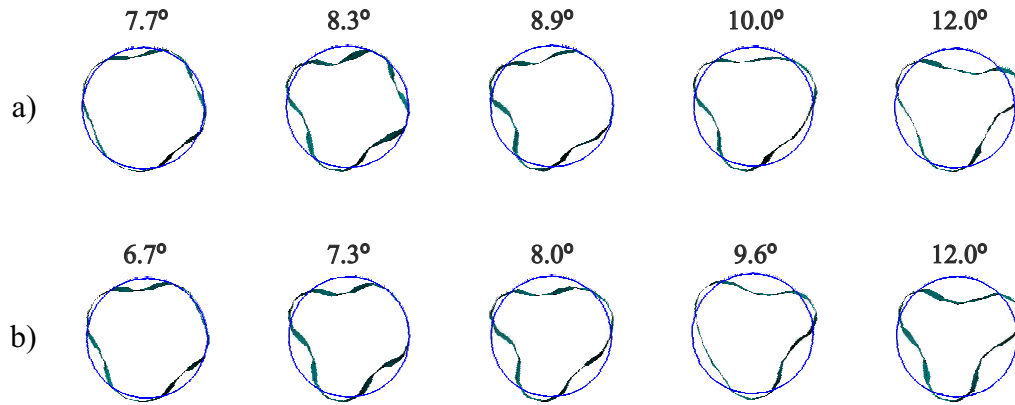
Fig. 9. Transformations of 4-half-wave post-buckling modes to 3-half-wave post-buckling modes (values of the twisting angle φ are given near the deformed configurations) obtained by solving the problem of twisting of the $(10, 10)$ armchair SWCNT under dynamic deformation for $\dot{\varphi} = 1.8\,°/\mathrm{ps}$ (see curves $\#3$ and $\#4$ in Fig. 4c d): a) type $\#9$ perturbations; b) type $\#10$ perturbations.

to be equal $\varphi = 15°$, and in the solution of the problem with perturbations (the authors do not mention the type of perturbations), the critical twisting angle was $\varphi = 9°$. In the present work (if by the solution of the problem with perturbations is meant the solution of the problem with perturbations of type $\#1$), similar critical values of the twisting angle were obtained (here by the critical angles in the solutions of the problem of quasi-static deformation of the nanotube, we mean the angles for which it was not possible to obtain converged deformed equilibrium configurations). The curve of the potential energy of internal forces V versus twisting angle φ obtained in the present work by solving the problem of post-buckling dynamic deformation of the nanotube with perturbations of type $\#1$ (see curve $\#2$ in Fig. 3a) is similar to the curve obtained in [4] by solving the problem of post-critical quasi-static deformation of the nanotube with perturbations (see the solid curve in Fig. 7 in [4]). The equilibrium configuration obtained by solving the problem of post-buckling deformation of the nanotube with perturbations for a twisting angle $\varphi = 25°$ is presented in Fig. 7 in [4]. This configuration corresponds to the fully flattened mode and is similar to the configurations obtained for this twisting angle in the present work with transformations of the helical 4-half-wave post-buckling modes into the fully flattened mode.

To summarize the comparison of the solutions obtained in [4] and in the present work, we note that in the present work, we reproduced the solutions presented in [4]. In addition, critical twisting angles corresponding to the singular points of integral curves were obtained. The fact that the obtained critical twisting angles are indeed the angles at which the nanotube can buckle is con-

firmed by a special choice of the type of perturbation whose introduction to the deformation process leads to buckling of the nanotube immediately after the twisting angles has reached the critical values. It is shown that with a special choice of the perturbations introduced into the solution of the problem of deformation of SWCNT and fitted to the 3-half-wave buckling mode, it is possible to obtain modes of post-critical deformation of the nanotube that are qualitatively different from the corresponding modes presented in [4].

4.2. Deformation and buckling of a (10,0) zigzag SWCNT

Consider a zigzag type SWCNT [40] with the chirality indices $(10, 0)$ of radius $R = 0.3931$ nm and length $L = 16.8980$ nm (79 hexagonal cells in its length) subjected to twisting with some prescribed atom displacements at its edges (see Fig. 2b). A solution of this problem is presented in a previous paper [1]. In the present paper, we obtain a more complete solution of this problem; in particular, we study the possibility of obtaining modes of deformed configurations for initial post-buckling deformation of the nanotube that correlate with the second buckling mode. In addition, we take into account the action of vdW forces in determining the post-critical deformation modes of the nanotube (in [1], vdW forces were neglected in determining these modes).

The atoms at the lower edge of the tube are constrained in the axial direction, while the atoms at the upper edge can move without constraints in this direction. In other respects, the formulation of the problem is similar to the formulation of the problem given in Sec. 4.1 and we, therefore, do not consider details of the strategy of solving the problem of twisting of the $(10, 0)$ zigzag SWCNT.

As a first step, we solved the unperturbed problem of quasi-static deformation of the SWCNT. Numerical experiments showed that the critical angle φ_{cr} corresponding to the first bifurcation point(s) of the integral curves (see Fig. 10a, b) is represented sufficiently accurately when integrating the equations of quasi-static deformation with a twisting angle step $\Delta\varphi = 0.1125°$. We find the first two bifurcation points on the integral curve for the dependence of the torque M on the twisting angle φ of the fundamental solution as follows: ($\varphi_{\mathrm{cr},1} = 18.338°$, $M_{\mathrm{cr},1} = 2.0698$ nN $\cdot$ nm) and ($\varphi_{\mathrm{cr},2} = 21.262°$, $M_{\mathrm{cr},2} = 2.3572$ nN $\cdot$ nm). These points correspond to the lower values of the twisting angle φ and the twisting moment M_1 in the intervals containing bifurcation points. The buckling modes of the nanotube obtained at these bifurcation points on the integral curve of the fundamental solution are depicted in Fig. 10c, d. We note that both buckling modes are 2-half-wave ones.

As in Sec. 4.1, by solutions of the unperturbed problem we mean solutions obtained in the case where the interatomic distances r_e for the initial configuration of the nanotube are specified with a minimum accuracy of 13 significant
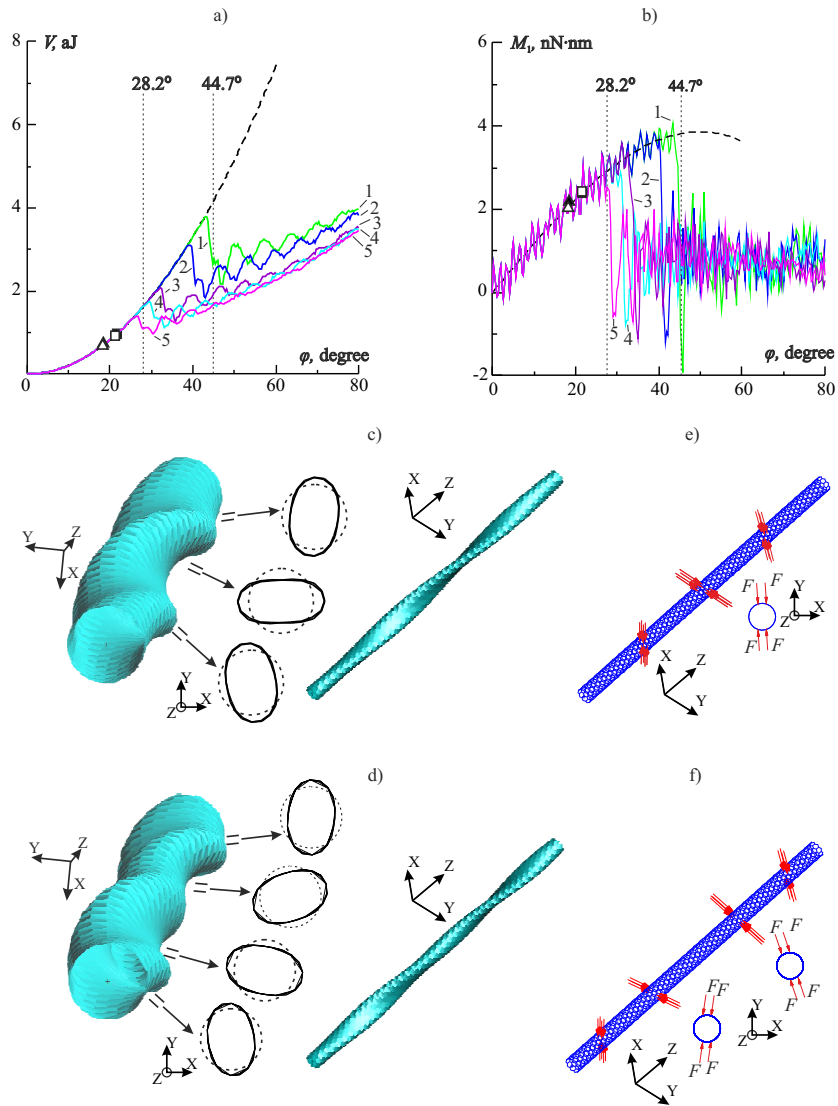
FIG. 10. Deformation and buckling of the twisted $(10, 0)$ zigzag SWCNT: a), b) potential energy of internal forces V and torque M_1 versus twisting angle φ (the dashed curves correspond to the solution of the quasi-static problem, and solid curves correspond to the solutions of dynamic problems for $\dot{\varphi} = 3.6\,°/\text{ps}$); solid curves #1 correspond to the solution of the unperturbed problem, and solid curves #2, #3, #4, and #5 correspond to the solutions of problems with perturbations of types #1, #2, #3, and #4; the '△' and '□' mark bifurcation points, and the '▲' and '■' mark the quasi-bifurcation points obtained in the solution of the unperturbed problem; c), d) the first and second buckling modes at the (quasi-)bifurcation points in the solution of the unperturbed problem; e) distribution of the perturbing compression forces acting on the atoms of the SWCNT and fitted to the buckling mode in c); f) distribution of the perturbing compression forces fitted to the buckling mode in d).

digits. By solutions of the problem with type #1 perturbation we understand solutions obtained for the initial positions of atoms in the nanostructure specified using up to the first five significant digits, and by solutions of problems with perturbations of types #2, #3, and #4 we understand solutions of problems obtained with specified additional compression forces applied to the atoms. These forces are fitted to the first (lower) buckling mode and have absolute values $F = 10^{-5}$, 10^{-4}, 10^{-3} nN, respectively (see Fig. 10e). In addition, by solutions of the problem with perturbations of types #5, #6, and #7 we mean solutions obtained with specified additional compression forces applied to the atoms in such a way that they are fitted to the second buckling mode and have absolute values $F = 10^{-5}$, 10^{-4}, 10^{-3} nN, respectively (see Fig. 10f).

Numerical experiments established that the deformation regime which is sufficiently extended in time occurs when the nanotube is twisted at a rate $\dot{\varphi} = 3.6\,°/\text{ps}$; in this case, the atoms at both edges of the nanotube make a full turn (i.e., $\varphi = 360°$) in a time $T = 100$ ps. To determine quasi-bifurcation points and the corresponding buckling modes, we performed a solution of the dynamic unperturbed problem (ignoring vdW forces) with the same step of the twisting angle ($\Delta\varphi = 0.1125°$) as in the similar quasi-static problem. As a result, we obtained quasi-bifurcation points that are close to the previously determined bifurcation points, namely, ($\varphi_{\text{cr},1} = 18.450°$, $M_{\text{cr},1} = 2.1751$ nN $\cdot$ nm) and ($\varphi_{\text{cr},2} = 21.375°$, $M_{\text{cr},2} = 2.3359$ nN $\cdot$ nm), and their corresponding buckling modes which coincide with the modes corresponding to the bifurcation points obtained in the solution of the problem of quasi-static deformation of the nanotube (see Fig. 10).

We found a time step $\Delta t = 0.00625$ ps with $\Delta\varphi = 0.0225°$ that ensured the convergence of the solutions up to a twisting angle of $360°$. The results of simulating the dynamic deformation of a twisted SWCNT for solving both the unperturbed problem and the problems with perturbations of types ##1–7 are depicted in Figs. 10–14.

As in Sec. 4.1, we observe two qualitatively different configuration modes of initial post-buckling deformation of the nanotube; that is, the configuration modes of initial post-buckling deformation obtained by solving the problem with perturbations of types #1, #2, #3, and #4 correlate with the first (lower) buckling mode presented in Fig. 10c (see the post-buckling configurations presented in Fig. 12a–d), and the configuration modes of initial post-buckling deformation obtained by solving the unperturbed problem and the problem with perturbations of types #5, #6, and #7 correlate with the second buckling mode presented in Fig. 10d (see the post-buckling configurations presented in Fig. 12e–h).

We note that the transformations of the initial post-buckling deformation modes correlated with buckling modes into the fully flattened modes that are obtained in this subsection differ from the similar transformations obtained in Sec. 4.1. For the SWCNT considered in Sec. 4.1, the transformations of the
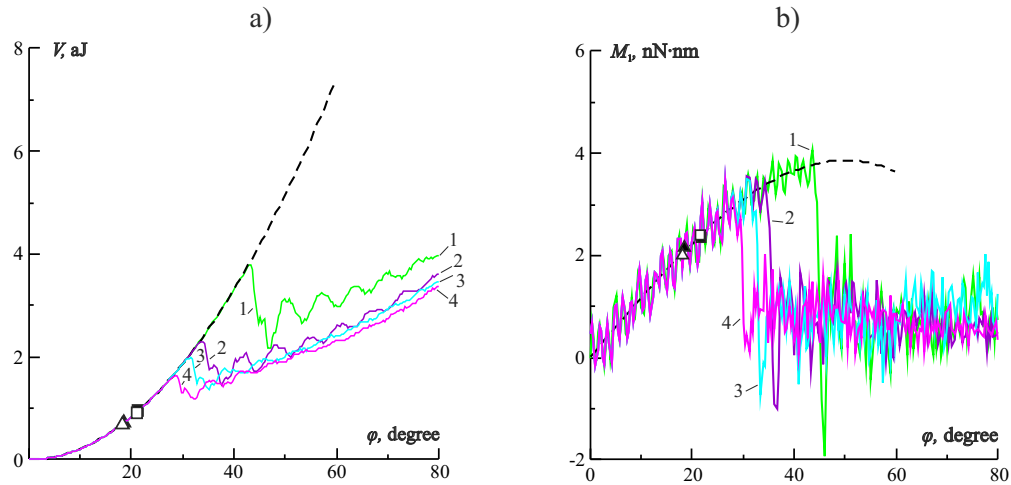
a)

b)

FIG. 11. Potential energy of internal forces V and torque M_1 versus twisting angle φ for the twisted $(10, 0)$ zigzag SWCNT (the dashed curves correspond to the solution of quasi-static problem, and solid curves correspond to the solutions of dynamic problems for $\dot{\varphi} = 3.6\,°/\text{ps}$): curves #1 correspond to the solution of the unperturbed problem, and curves #2, #3, and #4 correspond to the solutions of problems with perturbations of types #5, #6, and #7 (perturbing compression forces fitted to the second buckling mode, see Fig. 10f).

3- (or 4-)half-wave deformation modes to the fully flattened modes proceed in a rapid (catastrophic) manner, and for the SWCNT considered in the present section, these transformations proceed smoothly since for this SWCNT, the fully flattened modes are simply compressed (relative to the initial post-buckling modes) 2-half-wave deformation modes.

Although the curves of the potential energy of internal forces V and the torque M_1 versus twisting angle φ obtained from the solution of the unperturbed problem and the problem of nanotube twisting with different perturbations types agree qualitativley with each other (see Fig. 13), the evolution of deformed configurations of the SWCNT at large twisting angles can follow different scenarios. For example, the solutions of the unperturbed problem and problems with perturbations of type #4 yield similar curves (see Fig. 13a, b), but the evolution scenarios of their deformed configurations at twisting angles $\varphi \gtrsim 200°$ differ significantly from each other (see Fig. 14).

Let us compare the solutions obtained in the present work with the solutions of the same problem obtained in our previous study [1]. We see that the scenario of initial post-buckling deformation of the nanotube corresponding to the solution of the unperturbed problem obtained in the present work differs radically from the scenario of this deformation presented in the cited paper. This difference lies in the fact that the modes of initial post-buckling deformation of the nanotube obtained in the present work correlate with the buckling mode
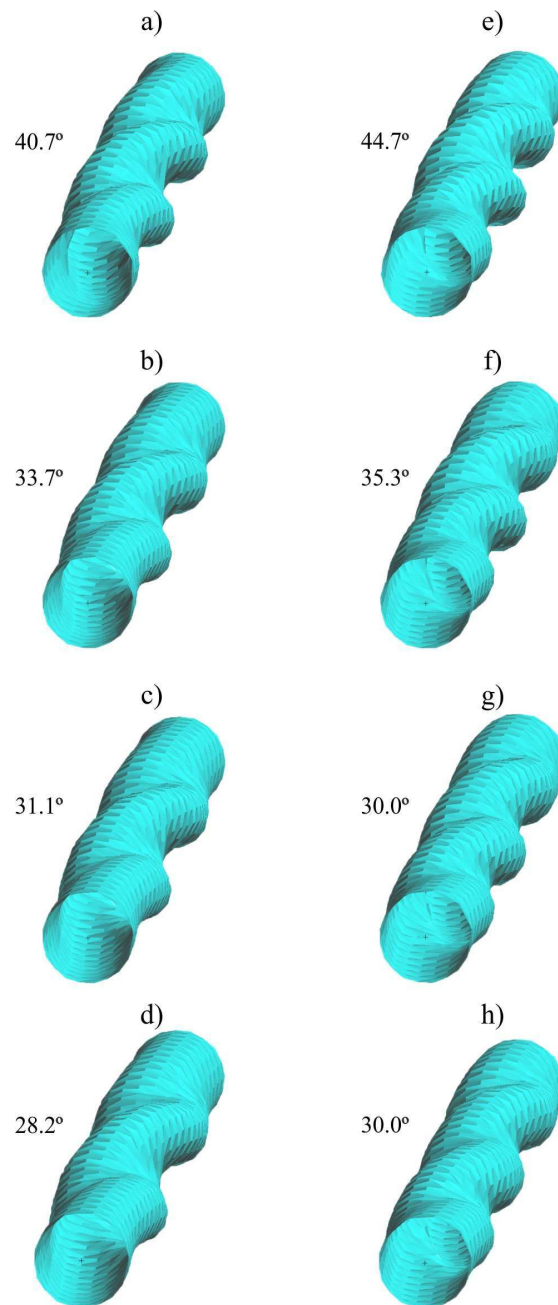
a)

40.7º

e)

44.7º

b)

33.7º

f)

35.3º

c)

31.1º

g)

30.0º

d)

28.2º

h)

30.0º

FIG. 12. Post-buckling configurations of the twisted $(10,0)$ zigzag SWCNT under dynamic deformation for $\dot{\varphi} = 3.6\,°/\text{ps}$ (values of the twisting angle φ are given near the deformed configurations) corresponding to the solutions of: a), b), c), d) problems with perturbations of types #1, #2, #3, and #4, respectively; e) the unperturbed problem; f), g), and h) problems with perturbations of types #5, #6, and #7, respectively.
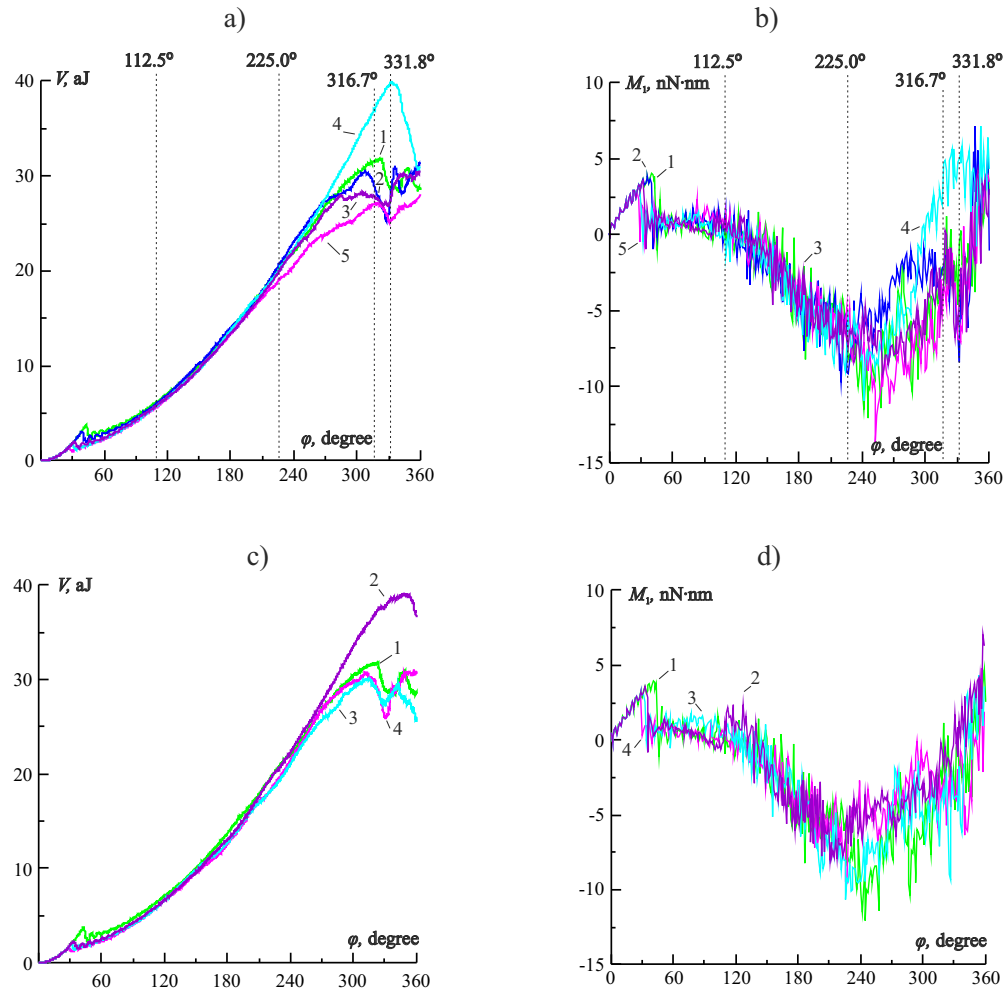
a)

b)

c)

d)

FIG. 13. Potential energy of internal forces V and the torque M_1 versus twisting angle φ for dynamic deformation of the twisted $(10, 0)$ zigzag SWCNT for $\dot{\varphi} = 3.6\,°/\text{ps}$. Curves #1 correspond to the solution of the unperturbed problem, and: a), b) curves #2, #3, #4, and #5 correspond to the solutions of the problem with perturbations of types #1, #2, #3, and #4, respectively; c), d) curves #2, #3, and #4 correspond to the solutions of the problem with perturbations of types #5, #6, and #7, respectively.

corresponding to the second (quasi-)bifurcation point, whereas in the solution presented in [1], these modes correlate with the buckling mode corresponding to the first (quasi-)bifurcation point. This difference cannot be caused to the inclusion of the vdW forces in the solution of the problem of post-critical deformation of the nanotube in the present work since for the initial post-buckling deformation of the nanotube, these forces are insignificant. The main reason for this large difference in the behavior of the solutions is the fact that in [1] an
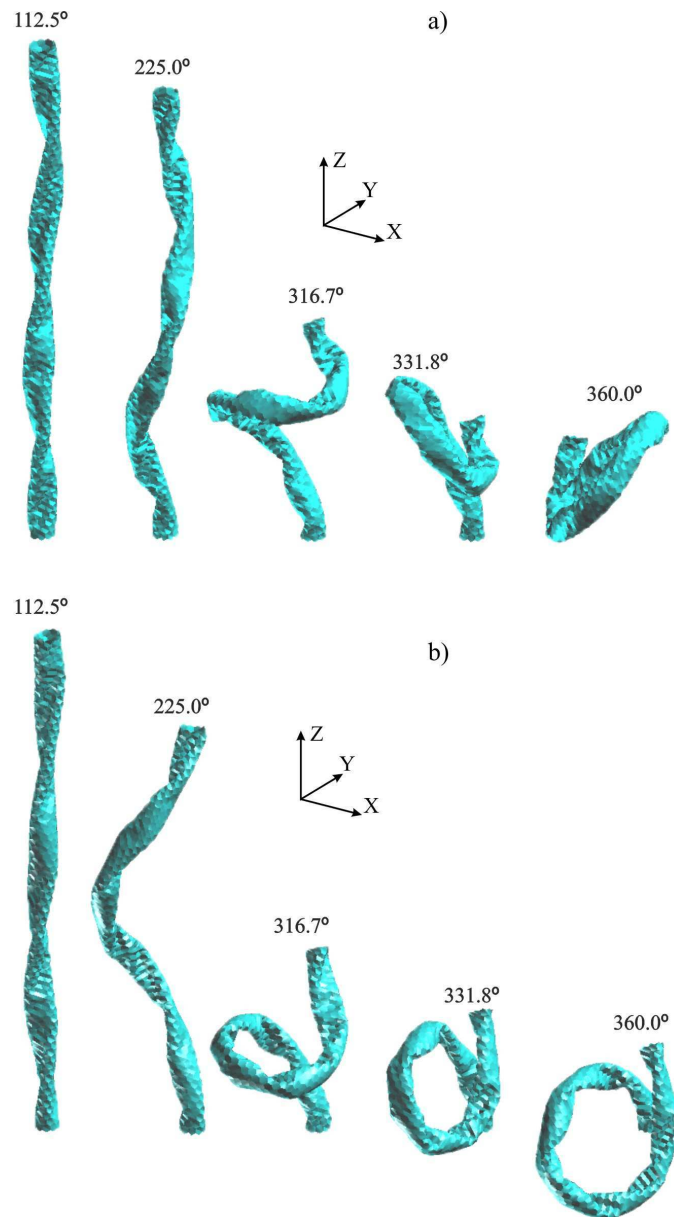
FIG. 14. Post-buckling configurations of the twisted $(10,0)$ zigzag SWCNT under dynamic deformation, obtained for $\dot{\varphi} = 3.6\,°/\text{ps}$ (values of the twisting angle φ are given near the deformed configurations): a) solution of the unperturbed problem; b) solution of the problem with type #4 perturbation.

underestimated (incorrectly determined) value of the mass of the carbon atom $(0.002029 \text{ nN·ps}^2/\text{nm}$ against $0.019927 \text{ nN·ps}^2/\text{nm}$ adopted in the present work), i.e., the inertial force is underestimated and the solution of the dynamic problem

obtained for deformation of the nanotube at a rate of twisting $\dot{\varphi} = 3.6\,°/\text{ps}$ is closer to the solution of the problem of quasi-static deformation of the nanotube than to the solution obtained in the present work at the same rate of twisting. This agrees with the fact that as the rate of twisting decreases to $0.36\,°/\text{ps}$ in the solution of the unperturbed problem, the integral curve of the numerical solution "branches" away from the integral curve of the fundamental solution at $\varphi = 23.428°^{4)}$, in contrast to the same "branching" at $\varphi = 43.425°$, obtained in the solution of the same problem with the rate of twisting $3.6\,°/\text{ps}$ (for the latter case, see Fig. 10a, b); in the solution of this problem presented in [1], the integral curve of the numerical solution "branches" away from the integral curve of fundamental solution at $\varphi = 29.137°$. In the solution of the unperturbed problem of deformation of the nanotube at a rate of twisting $0.36\,°/\text{ps}$, the modes of deformed configurations at initial post-critical motion of the nanotube correlate with buckling mode corresponding to the first quasi-bifurcation point, i.e., as the rate of twisting decreases from $3.6\,°/\text{ps}$ to $0.36\,°/\text{ps}$ the initial post-critical deformation of the nanotube follows a scenario close to the scenario presented in [1].

Another radical difference between the solutions of the problems given in the present work and the solutions of the same problems presented in [1] is that in [1] the vdW forces, which prevent the walls of the nanotube from being self-intersected, were neglected, and in the present work, these forces are taken into account. We note that the solutions of the nanotube twisting problem with and without taking into account the vdW forces give different equilibrium configurations for advanced post-critical deformation. For the post-critical deformation of the $(10, 0)$ SWCNT, the deformed configurations obtained in [1] resemble a "twisted candy wrapper", and the similar deformed configurations obtained in the present work resemble a "twisted ribbon" (fully flattened mode). This qualitative change in the modes of deformed configurations due to accounting for the vdW forces leads to the fact that mathematical models of twisted nanotubes taking into account the vdW forces become more flexible than models without the vdW forces. To recapitulate, we emphasize the significance of accounting for the vdW forces in determining modes of post-critical deformed configurations in solutions of nonlinear problems on buckling of twisted SWCNTs (see also [51]).

5. Conclusions

In the present work, numerical solution procedures based on the solution of nonlinear MM equations were developed for problems of quasi-static/dynamic deformation and buckling of nanostructures. An important advantage of these

---

$^{4)}$This solution is not given in the present work.

procedures over the solution of similar problems using the molecular dynamics method is that the interval of solution stability and buckling modes can be obtained only from the information contained in the fundamental solution.

The theoretical aspects worked out here were illustrated by solving the problems of twisting of SWCNTs. Assuming quasi-static deformation, we find the critical values of the torque and the buckling modes at the bifurcation points of the solutions of the problem without perturbations of the geometrical parameters and external forces. The same problem was solved as a dynamic problem for a nanotube twisting regime sufficiently extended in time. At a quasi-bifurcation point, buckling modes of the twisted nanotubes occurred which were close to the similar buckling modes for the quasi-static deformation. Therefore, the procedures used in this work to solve the nonlinear deformation problems enabled us to determine the critical states of the nanotubes simultaneously under both quasi-static and dynamic deformation conditions.

Acknowledgements

References

1. B.D. Annin, S.N. Korobeynikov, A.V. Babichev, *Computer simulation of a twisted nanotube buckling*, J. Appl. Ind. Math., **3**, 3, 318–333, 2009.

2. B.D. Annin, V.V. Alekhin, A.V. Babichev, S.N. Korobeynikov, *Computer simulation of nanotube contact*, Mech. Solids, **45**, 3, 352–369, 2010.

3. R. Ansari, S. Rouhi, *Atomistic finite element model for axial buckling of single-walled carbon nanotubes*, Physica E, **43**, 58–69, 2010.

4. M. Arroyo, T. Belytschko, *An atomistic-based finite deformation membrane for single layer crystalline films*, J. Mech. Phys. Solids, **50**, 1941–1977, 2002.

5. M. Arroyo, T. Belytschko, *A finite deformation membrane based on inter-atomic potentials for the transverse mechanics of nanotubes*, Mechanics of Materials, **35**, 3–6, 193–215, 2003.

6. A.V. Babichev, *Automating model construction and visualization of results of numerical simulation of deformation of nanostructures*, Comp. Cont. Mech., **1**, 4, 21–28, 2008 [in Russian].

7. K.-J. Bathe, *Finite Element Procedures*, Prentice Hall, Upper Saddle River, New Jersey, 1996.

8. R.C. Batra, S.S. Gupta, *Wall thickness and radial breathing modes of single-walled carbon nanotubes*, Trans. ASME. J. Appl. Mech., **75**, 061010, 2008.

9. T. Belytschko, S.P. Xiao, G.C. Schatz, R.S. Ruoff, *Atomistic simulations of nanotube fracture*, Phys. Rev. B, **65**, 235430, 2002.

10. N.G. Chopra, L.X. Benedict, V.H. Crespi, M.L. Cohen, S.G. Louie, A. Zettl, *Fully collapsed carbon nanotubes*, Nature, **377**, 135–138, 1995.

11. A. Curnier, *Computational Methods in Solid Mechanics*, Kluwer Academic Publ., Dordrecht, 1994.

12. P. Dlużewski, P. Traczykowski, *Numerical simulation of atomic positions in quantum dot by means of molecular statics*, Arch. Mech., **55**, 5–6, 393–406, 2003.

13. C.L. Dym, *Stability Theory and Its Applications to Structural Mechanics*, Noordhoff Int. Publ., Leyden 1974.

14. L.A. Elsgolts, *Differential Equations and Variational Calculus*, Nauka, Moscow 1969 [in Russian].

15. L.A. Girifalco, M. Hodak, R.S. Lee, *Carbon nanotubes, buckyballs, ropes, and a universal graphitic potential*, Phys. Rev. B, **62**, 19, 13104–13110, 2000.

16. R.V. Goldstein, A.V. Chentsov, *A discrete-continuous model of a nanotube*, Mech. Solids, **40**, 4, 45–59, 2005.

17. R.V. Goldstein, A.V. Chentsov, R.M. Kadushnikov, N.A. Shturkin, *Methodology and metrology for mechanical testing of nano-and microdimensional objects, materials, and products of nanotechnology*, Nanotechnologies in Russia, **3**, 1–2, 112–121, 2008.

18. S.S. Gupta, R.C. Batra, *Elastic properties and frequencies of free vibrations of single-layer graphene sheets*, Journal of Computational and Theoretical Nanoscience, **7**, 1–14, 2010.

19. N. Hu, K. Nunoya, D. Pan, T. Okabe, H. Fukanaga, *Prediction of buckling characteristics of carbon nanotubes*, Int. J. Solids Structures, **44**, 20, 6535–6550, 2007.

20. X. Huang, H. Yuan, W. Liang, S. Zhang, *Mechanical properties and deformation morphologies of covalently bridged multi-walled carbon nanotubes: Multiscale modeling*, J. Mech. Phys. Solids, **58**, 1847–1862, 2010.

21. Z. Kang, M. Li, Q. Tang, *Buckling behavior of carbon nanotube-based intramolecular junctions under compression: Molecular dynamics simulation and finite element analysis*, Computational Materials Science, **50**, 253–259, 2010.

22. A.R. Khoei, E. Ban, P. Banihashemi, M.J. Abdolhosseini Qomi, *Effects of temperature and torsion speed on torsional properties of single-walled carbon nanotubes*, Materials Science and Engineering C, **31**, 452–457, 2011.

23. M. Kleiber, W. Kotula, M. Saran, *Numerical analysis of dynamic quasi-bifurcation*, Engineering Computations, **4**, 1, 48–52, 1987.

24. S.N. Korobeinikov, V.P. Agapov, M.I. Bondarenko, A.N. Soldatkin, *The general purpose nonlinear finite element structural analysis program PIONER*, [in:] B. Sendov *et al.* [Eds.], Proc. Int. Conf. on Numerical Methods and Applications, Publ. House of the Bulgarian Acad. of Sci., Sofia, pp. 228–233, 1989.

25. S.N. Korobeynikov, *Application of finite element method for solving the nonlinear problems on deformation and buckling of atomic lattices*, Lavrentyev Institute of Hydrodynamics, Novosibirsk, Preprint No. 1-97, 1997 [in Russian].

26. S.N. KOROBEINIKOV, *The numerical solution of nonlinear problems on deformation and buckling of atomic lattices*, Int. J. Fracture, **128**, 1, 315–323, 2004.

27. S.N. KOROBEYNIKOV, *Nonlinear equations of deformation of atomic lattices*, Arch. Mech., **57**, 6, 457–475, 2005.

28. S.N. KOROBEYNIKOV, A.V. BABICHEV, *Numerical simulation of dynamic deformation and buckling of nanostructures*, [in:] R.V. GOLDSTEIN [Ed.], CD ICF Interquadrennial conference full papers, Moscow, Russia, 7–12 July, 2007, Institute for Problems in Mechanics, Moscow 2007.

29. W.B. KRÄTZIG, L.-Y. LI, *On rigorous stability conditions for dynamic quasi-bifurcations*, Int. J. Solids Structures, **29**, 1, 97–104, 1992.

30. W.B. KRÄTZIG, P. NAWROTZSKI, P. WRIGGERS, S. REESE, *Fundamentals of nonlinear instabilities and response analysis of discretized systems*, [in:] A.N. KOUNADIS, W.B. KRÄTZIG [Eds.], Nonlinear Stability of Structures (Theory and Computation Techniques), CISM Courses and Lectures No. 342, Springer, Wien, pp. 245–415, 1995.

31. A.M. KRIVTSOV, *Deformation and Failure of Solids with Microstructure*, Fizmatlit, Moscow 2007 [in Russian].

32. J. LA SALLE, S. LEFSCHETZ, *Stability by Liapunov's Direct Method with Applications*, Academic Press, New York, London 1961.

33. L.H.N. LEE, *On dynamic stability and quasi-bifurcation*, Int. J. Non-Linear Mech., **16**, 1, 79–87, 1981.

34. A.Y.T. LEUNG, X. GUO, X.Q. HE, H. JIANG, Y. HUANG, *Postbuckling of carbon nanotubes by atomic-scale finite element*, J. Appl. Phys., **99**, 124308, 2006.

35. C. LI, T.W. CHOU, *A structural mechanics approach for the analysis of carbon nanotubes*, Int. J. Solids Structures, **40**, 2487–2499, 2003.

36. B. LIU, Y. HUANG, H. JIANG, S. QU, K.C. HWANG, *The atomic-scale finite element method*, Comput. Methods Appl. Mech. Engrg., **193**, 1849–1864, 2004.

37. B. LIU, H. JIANG, Y. HUANG, S. QU, M.-F. YU, *Atomic-scale finite element method in multiscale computation with applications to carbon nanotubes*, Phys. Rev. B, **72**, 035435, 2005.

38. G.M. ODEGARD, T.S. GATES, L.M. NICHOLSON, E. WISE, *Equivalent-continuum modeling of nano-structured materials*, Composites Science and Technology, **62**(14), 1869–1880, 2002.

39. V. PARVANEH, M. SHARIATI, A.M.M. SABETI, *Investigation of vacancy defects effects on the buckling behavior of SWCNTs via a structural mechanics approach*, European Journal of Mechanics A/Solids, **28**, 1072–1078, 2009.

40. R. SAITO, M. FUJITA, G. DRESSELHAUS, M.S. DRESSELHAUS, *Electronic structure of chiral graphene tubules*, Appl. Phys. Lett. **60**, 18, 2204–2206, 1992.

41. A. SAKHAEE-POUR, *Elastic buckling of single-layered graphene sheet*, Computational Materials Science, **45**, 266–270, 2009.

42. A.R. SETOODEH, M. JAHANSHAHI, H. ATTARIANI, *Atomistic simulations of the buckling behavior of perfect and defective silicon carbide nanotubes*, Computational Materials Science, **47**, 388–397, 2009.

43. A. Shahabi, M. Ghassemi, S.M. Mirnouri Langroudi, H. Rezaei Nejad, M.H. Hamedi, *Effect of defect and C60s density variation on tensile and compressive properties of peapod*, Computational Materials Science, **50**, 586–594, 2010.

44. V.I. Shalashilin, E.B. Kuznetsov, *Parametric Continuation and Optimal Parametrization in Applied Mathematics and Mechanics*, Kluwer Academic Publ., Dordrecht 2003.

45. T. Sokol, M. Witkowski, *The equilibrium path determination in nonlinear analysis of structures*, [in:] M. Papadrakakis, B.H.V. Topping [Eds.], Advances in Non-linear Finite Element Methods: Proc. 2nd Int. Conf. on Computational Structures Technology, Civil-Comp Press, Edinburgh, pp. 35–45, 1994.

46. H.Y. Song, X.W. Zha, *Molecular dynamics study of effects of nickel coating on torsional behavior of single-walled carbon nanotube*, Physica B, **406**, 992–995, 2011.

47. J. Wackerfuss, *Molecular mechanics in the context of the finite element method*, Int. J. Num. Meth. Engng, **77**, 969–997, 2009.

48. C.M. Wang, Y.Y. Zhang, Y. Xiang, J.N. Reddy, *Recent studies on buckling of carbon nanotubes*, Appl. Mech. Reviews, **63**, 030804, 2010.

49. Z. Wang, D. Cheng, Z. Li, X. Zu, *Atomistic simulation of the torsional buckling of single-crystalline GaN nanotubes*, Physica E, **41**, 88–91, 2008.

50. Z. Waszczyszyn, C. Cichoń, M. Radwańska, *Stability of Structures by Finite Element Method*, Elsevier, Amsterdam 1994.

51. C.-L. Zhang, H.-S. Shen, *Buckling and postbuckling analysis of single-walled carbon nanotubes in thermal environments via molecular dynamics simulation*, Carbon, **44**, 13, 2608–2616, 2006.